UK Atomic
Energy
Authority

ExCALIBUR

Equations for ExCALIBUR/NEPTUNE Proxyapps

Version 1.26

Abstract

The report describes equations for ExCALIBUR project NEPTUNE Proxyapps, together with supporting information regarding Braginskii's transport coefficients and sources of atomic and molecular radiation. The numbering of the systems follows that of the NEPTUNE Science Plan, so that those listed under FM-WP2 are denoted 2-1, 2-2, etc., and under FM-WP3 as 3-1, 3-2, etc. It is a living document to which further equation systems will be added throughout the course of the
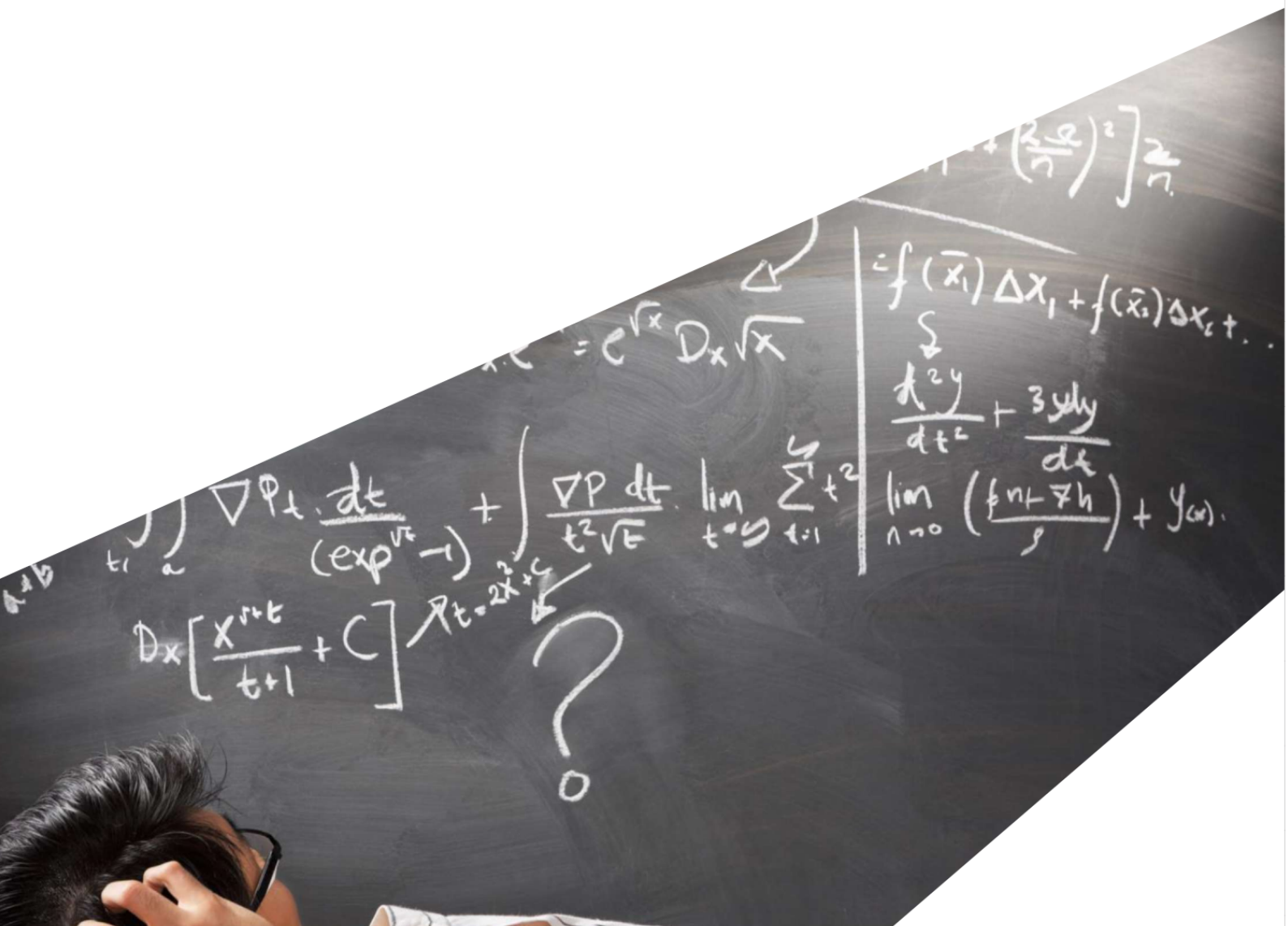
UKAEA REFERENCE AND APPROVAL SHEET

	Client Reference:	
	UKAEA Reference:	CD/EXCALIBUR-FMS/021
	Issue:	1.26
	Date:	14 March 2023
Project Name: ExCALIBUR Fusion Modelling System		

	Name and Department	Signature	Date
Prepared By:	Wayne Arter BD		14 March 2023
Reviewed By:	Rob Akers Advanced Computing Dept. Manager		14 March 2023
Approved By:	Rob Akers Advanced Computing Dept. Manager		14 March 2023

1 Introduction

Rather than attempting to develop a fully 3-D Exascale targeted plasma edge (or boundary) code from day one, project NEPTUNE will first focus upon the development of "proxyapps" [1], developed by partners across the project through a series of Grant calls. These must be designed and encoded to pave the way to the fully 3-D, actionable and performant NEPTUNE code (or codes) outlined in the Science Plan. As such, all NEPTUNE proxyapps must capture the functionality and performance/scalability characteristics of the eventual infrastructure as much as possible. In addition, all of the solutions across the NEPTUNE programme must eventually be synergistic, leading to an integrated solution for the eventual code(s) – this will require close cooperation through co-design across all partner organisations. The baseline proxyapps for the initial years of the project are described briefly in the Science Plan [2], and expanded upon below to give the "baseline plan" model equations, geometry and boundary conditions. Note, the baseline plan does not preclude additional functionality that any bidder may deem useful (or even essential) to the project. Bidders are encouraged in their response to calls to be creative and ambitious and to describe their own ideas and plans for delivering above and beyond core scope, provided the aim is to increase impact, quality, reduce risk and/or accelerate delivery (and that deliverables are fully aligned with the goals of the NEPTUNE Science Plan [2]).

At baseline, proxyapps target $x86$ (and ideally IBM POWER and ARM CPU) architectures (multi-core and multiple node) for scalability to first generation Exascale hardware. Proxyapps might also target other Exascale candidate architectures (eg. GPGPU) and/or demonstrate a capability to explore the use of novel hardware as it becomes available to the ExCALIBUR project as part of the novel test-bed programme. In order to execute efficiently on parallel architectures, proxyapps are expected to examine use of MPI, OpenMP or some other software technology (ideally with a focus upon performance portability).

Supporting information regarding Braginskii's transport coefficients for plasma in a strong magnetic field appears in Section 2. A description of sources of atomic and molecular radiation is given as an annex in Section A. A second annex Section B tabulates the mathematical symbols (with their units) used in the current document.

1.1 Overall Plan

In the Science Plan [2] the description of work extending beyond Y3 (early 2022) is deliberately vague on the subject of "gyrokinetics", as no widely accepted model for the tokamak edge appears to be available as of early Y2, and even should one appear, it might not be suitable for use in Y3 in NEPTUNE.

As listed, the proxyapps correspond to Plan A, which assumes that no suitable gyroaveraged model will emerge in time, hence *kinetic* implies Particle-in-Cell (PIC). PIC approaches, where charge conservation is vital to control errors, can anyway usefully be pursued for modelling low collisionality plasma species, and should simplify nicely to treat neutral species with long mean-free-paths in tokamak edge problems where mass conservation has been discovered to be critical. Moreover in the context of classical fluid dynamics, the transition from fluid to particles, or short to long mean-free-path, has been well-studied because of the application to the space vehicle

re-entry problem and related hypersonic situations. Thus the hybrid fluid/PIC approach might be regarded as a relatively low-risk route to achieving a robust numerical algorithm.

Evidently full-orbit PIC has the potential to be extremely inefficient relative to gyroaveraged kinetic theory because of the need to follow gyro-orbits in detail. Hence if this can be avoided, either through gyroaveraging or clever numerics or indeed a combination of both, then Plan B will see *kinetic* imply gyroaveraged kinetic theory for modelling plasma species in the proxyapps.

Regarding implementation at the Exascale there is also a conservative Plan A approach which sees the use of relatively simple data structures such as scalar and vector arrays to transfer data, and consequent use of existing code-coupling technologies. Plan B is an aggressive approach to implementation which sees custom data structures allowing for all physical data (particle arrays and fluid field vectors) colocated near a point to be held close in memory, permitting very tight custom code-coupling. As with the *kinetic* options, this Plan B promises significantly faster solutions than the corresponding Plan A, but its adoption depends on the outcome of research work to de-risk.

1.2 Proxyapps Summary

The overall thinking behind the proxyapps is to explore potential 'roadblocks' to the Exascale as early and in as simple a context as is possible, beginning with algorithmic roadblocks. NEPTUNE is directed towards producing 'actionable' code as the basis for large procurements, whereas more physics-focussed software projects conducted by the worldwide nuclear fusion have already advanced to greater complexity, minimising the risk that unexpected problems will appear in the full model.

The numbering of proxyapps below corresponds to the Science Plan.

2-1 2-D model of anisotropic heat transport. It is important to determine early the degree of anisotropy that high-order elements can treat without special coding. If this is unsatisfactorily small, then there are implications for geometry input as well as algorithmic developments that are best addressed as early as possible.

2-2 2-D elliptic solver in complex geometry. One of the indicated elliptic solvers is Grad-Shafranov to produce high order ('spectrally') accurate magnetic fields for use in many other proxyapps. Since Sovinec [3] has already produced a spectral element Grad-Shafranov code, the corresponding NEPTUNE development should mainly serve to identify practical issues concerning implementing high order fe models. The second solver additionally presents a chance to explore comparatively novel meshing techniques developed under Activity A2.1, and later the preconditioning techniques of A2.7.

2-3 1-D fluid solver with simplified physics but with UQ and realistic boundary conditions. This will determine the capability of spectral/hp element to handle sonic outflow boundary conditions needed to represent sheaths, together with large source terms, as well as identifying practical issues concerning intrusive UQ. This software is already potentially useful in its own right for example in modelling MAST-U divertor, and other workers might be drawn in to add additional physical effects to this end.

2-4 Spatially 1-D plasma model incorporating velocity space effects. From the numerical analytic point-of-view, this is a key demonstration of spectral/hp element capability to handle particle interactions. However, again this could be a basis for divertor modelling, to explore sheath effects depending on fieldline incidence on surface, and with minor modification the spread of particle energy around tile edges and corners as performed by Gunn et al [4, 5] for ITER application.

2-5 Spatially 1-D multispecies plasma model. Multispecies throws up a surprising number of issues concerning data definitions (eg. changes to the Coulomb logarithm), structures to deal with different number of species, and perhaps most significantly, complicated inter-species interaction terms both within and at the domain boundaries. This is also an opportunity to mix fluid and *kinetic* representations of *different* species within the *volume*.

2-6 Spatially 2-D plasma model incorporating velocity space effects. With the 1-D multispecies fluid work's having made the generalisation to 2-D straightforward, the challenge here is to start writing a complex proxyapp in production mode, incorporating the research put into design, documentation, code generation and benchmarking. There is an opportunity to study species with both fluid and *kinetic* representations depending on location relative to the wall. Again this is potentially a useful tool in its own right, capable of revealing deficiencies in previous 2-D modelling work.

2-7 Interaction between models of different dimensionality. This should verify that the design has the right data structures to handle additional further complexity beyond intrusive and ensemble-based UQ and model order reduction. The hopefully burgeoning NEPTUNE community could develop this into a design tool with a capability both to explore a large area of tokamak edge parameter space quickly in 0-D or 1-D and also to focus on relatively small but critical 2-D features, such as tile edges.

2-8 Spatially 3-D plasma *kinetic* models. These will represent the full fluid model produced by the 5-year NEPTUNE project, incorporating features of 2-D fluid and *kinetic* work in a 3-D code.

3-1 2-D particle-based model of neutral gas & impurities with critical physics. This will be a $2d3v$ code (ie. spatially 2-D distribution of particles with 3 velocity components) designed from the outset to interact with a high-order finite-element fluid model of plasma. It gives an opportunity to check out ideas on optimal usage of particles.

3-2 2-D moment-based model of neutral gas & impurities. Constructing a 2-D fluid code of neutral gas from the Nektar++ software should be a valuable educational exercise, whilst providing scope for cross-validating the 2-D particle model.

3-3 Interaction with 2-D plasma model when available. Building on the 1-D multispecies fluid work, the challenge here is to incorporate in the fluid code of Proxyapp PA2-6, particle effects from PA3-1, which will in the higher dimensional space be more subject to lack of numerical resolution or 'noise'. Should PA3-3 be accelerated, it could usefully treat both plasma and neutrals via particle models.

3-4 3-D model of neutral gas & impurities. This is now at full dimensional complexity, incorporating selected ideas on optimal usage of particles.

3-5 Interaction with 3-D plasma model. This will represent the full model produced by the 5-year NEPTUNE project, a coupling of fluid and *kinetic* software developed under the FM-WP2 work-package as PA2-8, incorporating features of Proxyapps 3-1 to 3-4, and allowing for additional input from PA3-6.

3-6 Staged introduction of additional neutral gas/impurity physics. It is expected that the NEP-TUNE community will join in to supplement the software with a wide-ranging capability to treat a wide range of additional nuclear, atomic and molecular effects.

2 Braginskii coefficients

Braginskii's transport coefficients are widely used in tokamak edge modelling. Object-oriented Fortran code to compute the Braginskii coefficients is available at the web-site [6].
Note that the constant k is introduced such that

$$k = k_B \ \text{ or } \ k = |e| \tag{1}$$

where k_B is Boltzmann's constant and $|e|$ is the unit of charge, depending whether T is measured in Kelvin or eV, so that kT is in energy units.

2.1 General

Except in Boltzmann's constant k_B, suffix B denotes a quantity from the Plasma Formulary [7]. See also Braginskii's paper [8]. The subsequent corrections by Epperlein and Haines, and by Mikhailovski and Tsypin are not relevant to this work.

In a magnetic field, the direction of which is given by unit vector $\mathbf{b}$, Goedbloed and Poedts [9] define three auxilliary vectors for a vector $\mathbf{v}$, viz.

$$\mathbf{v}_\parallel = \mathbf{b}(\mathbf{b} \cdot \mathbf{v}), \ \ \mathbf{v}_\wedge = \mathbf{b} \times \mathbf{v} \ \text{ and } \ \mathbf{v}_\perp = (\mathbf{b} \times \mathbf{v}) \times \mathbf{b} \tag{2}$$

If $\mathbf{v} = (v_1, v_2, v_\parallel)$ and $\mathbf{b}$ is aligned with the 3-axis in a Cartesian coordinate system, then

$$\mathbf{v}_\parallel = (0, 0, v_\parallel), \ \ \mathbf{v}_\wedge = (-v_2, v_1, 0) \ \text{ and } \ \mathbf{v}_\perp = (v_1, v_2, 0) \tag{3}$$

It may be shown that a tensor $\mathcal{T}$ which is symmetric under rotation about $\mathbf{b}$ has the form (in Cartesians)

$$\mathcal{T} = \begin{pmatrix} \mathcal{T}_\perp & -\mathcal{T}_\wedge & 0 \\ \mathcal{T}_\wedge & \mathcal{T}_\perp & 0 \\ 0 & 0 & \mathcal{T}_\parallel \end{pmatrix} \tag{4}$$

so that

$$\mathcal{T} \cdot \mathbf{v} = \mathcal{T}_\parallel \mathbf{v}_\parallel + \mathcal{T}_\wedge \mathbf{v}_\wedge + \mathcal{T}_\perp \mathbf{v}_\perp \tag{5}$$

2.2 Conduction, Viscous and Resistive Coefficients

The electron parallel thermal conductivity in the Braginskii theory is given as [7]

$$\mathcal{K}_{e\parallel} = 3.2 \frac{NkT_e}{m_e} \tau_e \tag{6}$$

a formula valid in either cgs or SI units, where τ_e is the electron relaxation time (measured in seconds), defined below. The notation is standard, with N the number density of electrons, approximately the same as the number density of ions, m_e the electron mass, and $T_\alpha, \quad s = i, e$ the temperature of species α. The perpendicular electron thermal conductivity satisfies similarly

$$\mathcal{K}_{e\perp} = 4.7 \frac{NkT_e}{m_e} \tau_e \cdot \frac{1}{(\omega_{ce}\tau_e)^2} \tag{7}$$

where the electron cyclotron frequency

$$\omega_{ce} = \frac{e}{m_e} \cdot B \tag{8}$$

Equivalent expressions for ions are

$$\mathcal{K}_{i\parallel} = 3.9 \frac{NkT_i}{m_i} \tau_i \tag{9}$$

$$\mathcal{K}_{i\perp} = 2 \frac{NkT_i}{m_i} \tau_i \cdot \frac{1}{(\omega_{ci}\tau_i)^2} \tag{10}$$

where the ion cyclotron frequency

$$\omega_{ci} = \frac{ZeB}{m_i} = \frac{e}{m_p} \cdot \frac{ZB}{A} \tag{11}$$

where Z is the charge state of the ion and A its atomic mass. The definitions above have to be interpreted in the context of the equations given in [7], so that thermal diffusivities are obtained by dividing by $3n_\alpha/2$ where $\alpha = i, e$ is the species index. It is also convenient to introduce the dimensionless factors

$$x_e = \omega_{ce}\tau_e \tag{12}$$

$$x_i = \omega_{ci}\tau_i \tag{13}$$

Kinematic viscosities in the Braginskii theory may be taken as

$$\nu_{e\parallel} = 0.73 NkT_e\tau_e/(Nm_e) = 0.73 \frac{kT_e}{m_e} \tau_e \tag{14}$$

$$\nu_{e\perp} = 0.51 NkT_e\tau_e/(Nm_e)\frac{1}{x_e^2} = 0.51 \frac{kT_e}{m_e} \tau_e \frac{1}{x_e^2} \tag{15}$$

$$\nu_{i\parallel} = 0.96 NkT_i\tau_i/(Nm_i) = 0.96 \frac{kT_i}{m_i} \tau_i \tag{16}$$

$$\nu_{i\perp} = 0.3 NkT_i\tau_i/(Nm_i)\frac{1}{x_i^2} = 0.3 \frac{kT_i}{m_i} \tau_i \frac{1}{x_i^2} \tag{17}$$

Key quantities in the calculation of all these terms are τ_α, $\alpha = i, e$. The first step in their calculation is to convert their formulas, usually given in cgs, to SI units, giving

$$\tau_e = 6\sqrt{2\pi^3}\frac{\epsilon_0^2\sqrt{m_e}}{e^4}\frac{(kT_e)^{3/2}}{Z^2 N\Lambda} = 3.44 \times 10^{-7}\frac{(T_e)^{3/2}}{Z^2(N/10^{18})\Lambda} \tag{18}$$

$$\tau_i = 12\sqrt{\pi^3}\frac{\epsilon_0^2\sqrt{m_p}}{e^4}\frac{(kT_i)^{3/2}\sqrt{A}}{Z^4 N\Lambda} = 2.09 \times 10^{-5}\frac{(T_i)^{3/2}\sqrt{A}}{Z^4(N/10^{18})\Lambda} \tag{19}$$

where the notation is standard with T_e and T_i measured in eV, except possibly the use of Λ for the Coulomb logarithm. The above check with expressions in Wesson [10, § 14]. Note that $Z^2\tau_i$ differs from τ_e in being larger by a factor of $\sqrt{2m_i/m_e} \approx 60\sqrt{A}$ (also substituting T_i for T_e is necessary). The factors in Z are taken from the original Braginskii paper [8].

It follows that the x_α factors may be conveniently written

$$x_e = 6.05 \times 10^4 \frac{(T_e)^{3/2}B}{Z^2(N/10^{18})\Lambda} \tag{20}$$

$$x_i = 1997\frac{(T_i)^{3/2}B}{Z^3(N/10^{18})\sqrt{A}\Lambda} \tag{21}$$

The large coefficients in Equations(20) and (21) explain why classical transport is so anisotropic.

Substituting the explicit expression for τ_e in Equations(6) and (9) gives respectively, the thermal parallel diffusivities are

$$\kappa_{e\parallel} = 13\sqrt{2\pi^3}\frac{1}{\sqrt{m_e}}\frac{\epsilon_0^2}{e^4}\cdot\frac{(kT_e)^{5/2}}{Z^2 N\Lambda} \tag{22}$$

$$\kappa_{i\parallel} = 16\sqrt{\pi^3}\frac{1}{\sqrt{m_p}}\frac{\epsilon_0^2}{e^4}\cdot\frac{(kT_i)^{5/2}}{Z^4 N\Lambda\sqrt{A}} \tag{23}$$

and the ratios are

$$x_e = \frac{6\sqrt{2\pi^3}\epsilon_0^2}{\sqrt{m_e}e^3}\cdot\frac{(kT_e)^{3/2}B}{Z^2 N\Lambda} \tag{24}$$

$$x_i = \frac{12\sqrt{\pi^3}\epsilon_0^2}{\sqrt{m_p}e^3}\cdot\frac{(kT_i)^{3/2}B}{Z^3 N\Lambda\sqrt{A}} \tag{25}$$

An expression for the perpendicular ion conductivity, maintaining the fixed physical factors is of interest

$$\kappa_{i\perp} = \frac{e^2\sqrt{m_p}}{9\sqrt{\pi^3}\epsilon_0^2}\cdot\frac{Z^2 N\Lambda\sqrt{A}}{(kT_i)^{1/2}B^2} \tag{26}$$

Assuming T_i is measured in eV, and N in units of $10^{18}\,\text{m}^{-3}$, then

$$\kappa_{i\perp} = 6.67 \times 10^{-4}\cdot\frac{Z^2(N/10^{18})\Lambda\sqrt{A}}{(T_i)^{1/2}B^2}\ \ m^2 s^{-1} \tag{27}$$

and

$$\kappa_{e\perp} = 5.26 \times 10^{-5}\cdot\frac{Z^2(N/10^{18})\Lambda}{(T_e)^{1/2}B^2}\ \ m^2 s^{-1} \tag{28}$$

The plasma resistivity is taken as

$$\eta = \eta_B/\mu_0 = \frac{0.51\sqrt{m_e}e^2}{6\sqrt{2\pi^3}\mu_0\epsilon_0^2} \cdot \frac{Z\Lambda}{(kT_e)^{3/2}} \tag{29}$$

Assuming T_e is measured in eV, then

$$\eta = \eta_B/\mu_0 = 41.9 \cdot \frac{Z\Lambda}{(T_e)^{3/2}} \ m^2 s^{-1} \tag{30}$$

2.3 Prandtl Numbers

The above expressions (except for the resistivity) apply strictly only when there are separate equations for ion and electron transport, so decisions have to be taken about how to combine the transport coefficients to treat the plasma as a single fluid. For the thermal transport, since pressures $p_e \approx p_i$, it is sufficient to add the κ_α. However, the values for ions and electrons are so disparate because $m_p \gg m_e$ that one or other might be neglected, assuming B is of order unity (in Tesla) and $T_e \approx T_i$, thus $\kappa_{e\parallel} \gg \kappa_{i\parallel}$ and hence $\kappa_\parallel \approx \kappa_{e\parallel}$, since

$$\left(\frac{x_i}{x_e}\right)^2 = \frac{2m_e}{Z^2 A m_p}\left(\frac{T_i}{T_e}\right)^3 \tag{31}$$

It also follows that

$$\frac{\kappa_{e\perp}}{\kappa_{i\perp}} = 0.078\left(\frac{T_i}{T_e}\right)^{1/2}\frac{1}{\sqrt{A}} \tag{32}$$

thus $\kappa_\perp \approx \kappa_{i\perp}$. There is the caveat that if T_i is approximately spatially constant radially, then $\kappa_{e\perp}$ might become relevant.

As for viscosity, since the ion momentum is so much greater than the electron momentum, then $\nu \approx \nu_i$.

For interchange motions where flows are perpendicular to the field, take $\kappa = \kappa_{i\perp}$, then on the *Cambridge* definition, the magnetic Prandtl number is

$$\zeta = \frac{\eta}{\kappa_{i\perp}} = \frac{0.765}{\sqrt{2}}\frac{1}{\mu_0}\sqrt{\frac{m_e}{m_p}} \cdot \frac{B^2}{ZN\sqrt{A}}\frac{(kT_i)^{1/2}}{(kT_e)^{3/2}} \tag{33}$$

which evaluates as (T_α in eV, N in units of $10^{18}\,\mathrm{m}^{-3}$)

$$\zeta = \frac{\eta}{\kappa_{i\perp}} = 62\,700 \cdot \frac{B^2}{Z(N/10^{18})\sqrt{A}}\frac{(T_i)^{1/2}}{(T_e)^{3/2}} \tag{34}$$

It may be argued that it is more appropriate to use the 'anomalous' value of $1\,m^2 s^{-1}$, in which case Equation (30) without units gives the 'Cambridge' magnetic Prandtl number.

The usual (viscous) Prandtl number is

$$Pr = \frac{\nu_{i\perp}}{\kappa_{i\perp}} = 0.23 \tag{35}$$

Note that P.H.Roberts [11] defines the magnetic Prandtl number as $Pr_M = \nu/\eta = Pr/\zeta$, and his definition is more widely used.

2.4 Using Braginskii and Other Coefficients

2.4.1 Introduction

The Branginskii coefficients might be used in a multispecies context over a range of different timescales. Ultimately finite element codes, indeed most numerical schemes, depend on solution of a linear algebra problem

$$A\mathbf{x} = \mathbf{b} \tag{36}$$

where $\mathbf{x}$ are field values to be determined, and A and $\mathbf{b}$ follow from the model. Take the simplest case of a 2×2 model

$$A = \begin{pmatrix} a_{11} & a_{12} \\ a_{21} & a_{22} \end{pmatrix}, \quad \mathbf{b} = (b_1 \ b_2)^T, \quad \mathbf{x} = (x_1 \ x_2)^T \tag{37}$$

where the demands of multispecies and multiscale may lead to widely different values of all coefficients and unknowns. To make these values comparable, which is desirable from the numerical standpoint, exploit the fact that it is possible to multiply each each equation separately without changing the value of the solution $\mathbf{x}$. Further, provided the coefficients a_{ij} are appropriately adjusted, each component x_j of $\mathbf{x}$ may be scaled separately. Thus

$$\begin{pmatrix} a_{11} & a_{12} \\ a_{21} & a_{22} \end{pmatrix} \begin{pmatrix} x_1 \\ x_2 \end{pmatrix} = \begin{pmatrix} b_1 \\ b_2 \end{pmatrix} \tag{38}$$

and

$$\begin{pmatrix} s_1 a_{11} t_1 & s_1 a_{12} t_2 \\ s_2 a_{21} t_1 & s_2 a_{22} t_2 \end{pmatrix} \begin{pmatrix} \tilde{x}_1 \\ \tilde{x}_2 \end{pmatrix} = \begin{pmatrix} \tilde{b}_1 \\ \tilde{b}_2 \end{pmatrix} \tag{39}$$

where

$$\tilde{\mathbf{x}} = (x_1/t_1 \ x_2/t_2)^T, \quad \tilde{\mathbf{b}} = (s_1 b_1 \ s_2 b_2)^T \tag{40}$$

give the same $\mathbf{x}$, although likely by solving equations with very different sized coefficients for very different sized unknowns $\tilde{\mathbf{x}}$. This approach is written more elegantly in matrix notation as

$$SAT^{-1}T\tilde{\mathbf{x}} = S\tilde{\mathbf{b}} \tag{41}$$

where S and T are diagonal matrices

$$S = \begin{pmatrix} s_1 & 0 \\ 0 & s_2 \end{pmatrix}, \quad T = \begin{pmatrix} 1/t_1 & 0 \\ 0 & 1/t_2 \end{pmatrix} \tag{42}$$

(so that T may be viewed as an elementary preconditioner).

Scaling each row of the matrix and each unknown becomes very expensive for a nonlinear and/or timestepping problem where A and $\mathbf{b}$ are large and continually changing. Thus it is helpful on this account only to scale by equation subsystem and by field, where by subsystem is meant eg. momentum balance for species X, and field is meant say number density of the coupled species Y. Hence it is convenient to regard x_1 as corresponding to an entire vector of discrete values of the number density of species X and x_2 similarly to represent the density of species Y, so that the coefficients a_{ij} for each i and each j separately represent a possibly very large matrix. Such a

grouping is convenient for making the equations dimensionless, in that s_1 may compensate for the dimensions of the equation

$$a_{11}x_1 + a_{12}x_2 = b_1 \tag{43}$$

and s_2 for the dimensions of

$$a_{21}x_1 + a_{22}x_2 = b_2 \tag{44}$$

whereas t_j may serve make dimensionless x_j for each $j = 1,\ 2$. There should be a reduced, hopefully avoidable, need to rescale equations as fields evolve, and properly dimensioned values should be easily restored as needed.

2.4.2 Fluid Models

In the above context, there is no need, having evaluated the Braginskii coefficients to convert them to non-dimensional form. Selected terms from the energy evolution equation demonstrate how the above scalings are to implemented in practice. Most likely, an equation for energy evolution would be considered instead of one divided by m_i, and for demonstration purposes, the factor of B can be omitted from System 2-3. The following terms in the energy evolution equation are representative

$$\frac{\partial}{\partial t}\left(\frac{3}{2}(NkT_d)\right) + \ldots = N\frac{\partial}{\partial s_\parallel}\kappa_{e\parallel}\frac{\partial kT_e}{\partial s_\parallel} + \ldots \tag{45}$$

The overall scaling of this equation to render its terms dimensionless is evidently $\frac{t_s}{kT_s} \cdot \frac{L_s^3}{N_{ref}}$ and the unknowns to be solved for, T_d and N, have respectively dimensions/scalings T_s and $\frac{L_s^3}{N_{ref}}$. The time dependent term in Equation (45) involves both unknowns, hence needs re-expressing as

$$\frac{\partial}{\partial t}\left(\frac{3}{2}(NkT_d)\right) = \frac{3}{2}Nk\frac{\partial T_d}{\partial t} + \frac{3}{2}kT_d\frac{\partial N}{\partial t} \tag{46}$$

so that $\frac{3}{2}Nk$ and $\frac{3}{2}kT_d$ are equivalents of coefficients a_T and a_N of matrix A. The partial derivative $\partial/\partial t$ leads to discrete operators $\tilde{\Delta}_t/\Delta t$ where $\tilde{\Delta}_t$ is a (dimensionless) difference operator so the scaling factorisations see

$$\frac{\frac{3}{2}Nk}{\Delta t}\tilde{\Delta}_t(T) \rightarrow \frac{L_s^3 t_s}{N_{ref}kT_s} \cdot \frac{\frac{3}{2}Nk}{\Delta t} \cdot T_s\tilde{\Delta}_t\left(\frac{T}{T_s}\right) \tag{47}$$

and

$$\frac{\frac{3}{2}kT_d}{\Delta t}\tilde{\Delta}_t(N) \rightarrow \frac{L_s^3 t_s}{N_{ref}kT_s} \cdot \frac{\frac{3}{2}kT_d}{\Delta t} \cdot \frac{N_{ref}}{L_s^3}\tilde{\Delta}_t(n) \tag{48}$$

where $\tilde{\Delta}_t$ operates on unknowns of dimensionless temperature T/T_s and density $n = L_s^3 N/N_{ref}$ respectively. The partial derivative $\partial^2/\partial s_\parallel^2$ leads to a discrete operator $\tilde{\Delta}_s^2/(\Delta s_\parallel)^2$ where $\tilde{\Delta}_s$ is a (dimensionless) difference operator so the scaling factorisation for a_κ is

$$\frac{L_s^3 t_s}{N_{ref}kT_s} \cdot \frac{Nk\kappa_{e\parallel}}{(\Delta s_\parallel)^2} \cdot T_s\tilde{\Delta}_s^2\left(\frac{T}{T_s}\right) \tag{49}$$

where $\tilde{\Delta}_s^2$ operates on the unknown of dimensionless temperature T/T_s.

The algorithm above producing the scaled matrix coefficients involves multiplying 3 factors together. If T is measured in eV, then $k = |e|$. Suppose $L_s = 10\,\mathrm{m}$ and $t_s = L_s/10^5\,m s^{-1} = 10^{-4}\,s$, $N = 10^{16}\,m^{-3}$, $T = 10\,eV$, and approximating $|e| \to 10^{-19}$, $3/2 \to 1$, taking $\Delta t = 0.1 t_s$ and $\Delta s_{\parallel} = 0.1 L_s$, then numerically

$$\frac{L_s^3 t_s}{N_{ref} k T_s} \cdot \frac{N k}{\Delta t} \cdot T_s \to 10^{3-4-18+19-2} \cdot 10^{-19+16+5} \cdot 10^2 \tag{50}$$

$$\frac{L_s^3 t_s}{N_{ref} k T_s} \cdot \frac{k T_d}{\Delta t} \cdot \frac{N_{ref}}{L_s^3} \to 10^{3-4-18+19-2} \cdot 10^{-19+1+5} \cdot 10^{18-3} \tag{51}$$

$$\frac{L_s^3 t_s}{N_{ref} k T_s} \cdot \frac{N k \kappa_{e\parallel}}{(\Delta s_{\parallel})^2} \cdot T_s \to 10^{3-4-18+19-2} \cdot 10^{16-19} \kappa_{e\parallel} \cdot 10^2 \tag{52}$$

so that each factor is not unmanageably different from unity when using single precision arithmetic. (The largest numerical value is 10^{15} if $\kappa_{e\parallel}$ is estimated as $10^9\,m^2 s^{-1}$.)

Ultimately, the scaled values of the coefficients a_T, a_N and a_κ are easily shown to be equal to respectively

$$\tilde{a}_T = \frac{t_s n}{\Delta t}, \quad \tilde{a}_N = \frac{t_s}{\Delta t} \frac{T_d}{T_s}, \quad \tilde{a}_\kappa = \frac{t_s \kappa_{e\parallel}}{(\Delta s_{\parallel})^2} n \tag{53}$$

which are all evidently of order unity.

If it is necessary to iterate to a solution for T_e or T_i, then the coefficient should be evaluated for $T = T_s$. For example $\kappa_{e\parallel}$, which varies proportional to $T^{5/2}$, should be evaluated as

$$\kappa_{e\parallel}(T) = \kappa_{e\parallel}(T_s) \left(\frac{T}{T_s} \right)^{\frac{5}{2}} \tag{54}$$

and then any further work, for example linearisation, may proceed using the dimensionless group T/T_s.

2.4.3 Scalings for Particle Models

The above considerations also apply in the case of particle evolution. Given the choice of units, if the equations of motion are posed in terms of superparticles of weight w_p,

$$w_p m_\alpha \frac{d\mathbf{v}}{dt} = w_p q_\alpha (\mathbf{E} + \mathbf{v} \times \mathbf{B}) \tag{55}$$

It is convenient to introduce a reference particle weight w_{ref}, cf. N_{ref}, to make scalings more manageable numerically. The overall equation scaling to render the terms dimensionless is then evidently $\frac{t_s}{w_{ref} m_u} \cdot \frac{t_s}{L_s} = \frac{t_s^2}{w_{ref} L_s m_u}$ and the unknown to be solved for, namely $\mathbf{v}$, has dimensions $\frac{L_s}{t_s}$. Consider the acceleration in Equation (55), which leads to discrete coefficient terms of the form $\frac{m_\alpha}{\Delta t}$, then the scaling factorisation is

$$\frac{w_p m_\alpha}{\Delta t} \mathbf{v} \to \frac{t_s^2}{L_s w_{ref} m_u} \cdot \frac{w_p m_\alpha}{\Delta t} \cdot \frac{L_s}{t_s} \tag{56}$$

to be applied to dimensionless velocity

$$\mathbf{v} \to \frac{t_s}{L_s}\mathbf{v} \tag{57}$$

As explained above, the numerical values of the 3 factors should be estimated. For definiteness, suppose $|\mathbf{v}| = 10^5\,ms^{-1}$, $B = 1\,\text{T}$, then the gyro-radius is approx. $10^{-3}\,m$. so take $L_s = 10^{-3}$ m as a typical lengthscale, then $t_s = 10^{-3-5} = 10^{-8}$ s, and a timestep size Δt of order 10^{-9} is indicated. Approximate the amu$\to 10^{-27}$ kg, and if $A = Z = 1$ and suppose $w_p = w_{ref} = 10^{10}$, the resulting factors follow as

$$\frac{t_s^2}{L_s w_{ref} m_u} \cdot \frac{w_p m_\alpha}{\Delta t} \cdot \frac{L_s}{t_s} \to 10^{-16+3-10+27} \cdot 10^{10-27+9} \cdot 10^{-3+8} \tag{58}$$

so that each factor is not unmanageably different from unity when using single precision arithmetic. (The smallest numerical value is 10^{-8}.)

The scaled coefficient is easily shown to simplify as

$$\tilde{a} = \frac{t_s^2}{w_{ref} m_u L_s} \cdot \frac{w_p m_\alpha}{\Delta t} \cdot \frac{L_s}{t_s} = \frac{t_s A}{\Delta t} \tag{59}$$

if $w_{ref} = w_p$, which is clearly of order unity. Evidently $\tilde{a}$ is of order the number of timesteps chosen to discretise a gyro-period, typically a number of order unity. The magnetic field term may similarly be treated

$$w_p|q_\alpha \mathbf{v} \times \mathbf{B}| \to \frac{t_s^2}{L_s w_{ref} m_u} \cdot w_p|q_\alpha|B \cdot \frac{L_s}{t_s} \tag{60}$$

whence

$$\frac{t_s^2}{L_s w_{ref} m_u} \cdot w_p|q_\alpha|B \cdot \frac{L_s}{t_s} \to 10^{-16+3-10+27} \cdot 10^{10-19} \cdot 10^5 \tag{61}$$

ie. the smallest numerical factor is 10^{-9}, and

$$\tilde{a} = t_s Z K_M|B| \approx 10^{-8+8} = 10^0 = 1 \tag{62}$$

3 System 2-1: 2-D model of anisotropic heat transport

The model for time evolution of the temperature field T is thermal diffusion, which in a plasma gives

$$\frac{3}{2}N\frac{\partial T}{\partial t} = \nabla \cdot \mathcal{K}\nabla T \tag{63}$$

where the thermal conductivity tensor is $\mathcal{K}$. (Compare the model for a solid

$$\rho_m c_p \frac{\partial T}{\partial t} = \nabla \cdot k_c \nabla T \tag{64}$$

where the thermal conductivity tensor is k_c, ρ_m is the mass density of the medium and c_p is its specific heat at constant pressure, implying that the thermal diffusivity tensor is $\kappa = k_c/\rho_m c_p$.) Introducing vector components as in Section 1, thermal diffusion in a plasma after Braginskii is thus

$$\frac{3}{2}N\frac{\partial T}{\partial t} = \nabla \cdot \left(\mathcal{K}_\parallel \mathbf{b}[\mathbf{b}.\nabla T] + \mathcal{K}_\perp (\nabla T - \mathbf{b}[\mathbf{b}.\nabla T]) + \mathcal{K}_\wedge \mathbf{b} \times \nabla T \right) \tag{65}$$

Henceforth, the 'wedge' transport ie. in due to the term in $\mathcal{K}_\wedge$ is neglected for the reason that it may be rearranged to give a convection-like term, via the identity

$$\nabla \cdot \mathcal{K}_\wedge \mathbf{b} \times \nabla T = \nabla \cdot (\mathbf{u}_\wedge T) \tag{66}$$

where

$$\mathbf{u}_\wedge = \nabla \times (\mathcal{K}_\wedge \mathbf{b}) \tag{67}$$

(In any event, if $\mathcal{K}_\wedge$ is a function purely of T, and $\nabla \cdot \mathbf{b} = \mathbf{0}$, then the terms in Equation (66) vanish.)

Expressions for the thermal diffusivities $\kappa_\perp$ and $\kappa_\parallel$ for the different species are given in Section 2.2, where they incorporate the factor $\frac{3}{2}N$, ie. $\kappa_{(\perp,\parallel)e,i} = \mathcal{K}_{(\perp,\parallel)}/(\frac{3}{2}N)$.

3.1 Test Cases

The aim of the work is to calculate in a series of calculations that increasingly approach the realistic model, the magnitude of the spurious numerical diffusion perpendicular to the magnetic field direction $\mathbf{b}$. The main interest concerns how much diffuses in the plasma, not the solid surface, even though the deposition of power is on the surface, reason: all sorts of complicated extra physics come into play in the plasma especially near surfaces.

3.1.1 Starting Case

For the 2-D test case illustrated in Figure 1, it is suggested that $\kappa_\perp = 0$ so that any perpendicular diffusion is numerical in origin. Given this, the problem can be analysed using any spatial scale and any convenient $\kappa_\parallel$. However an order of magnitude estimate for tile dimensions is one metre, discharge timescale is one second upwards. For plasma properties assume $N = 10^{18}\,\text{m}^{-3}$, $T_i = T_e = 10\,\text{eV}$, $Z = A = 1$, $B = 3\,\text{T}$ and solid temperatures say $500^o\,\text{C}$.
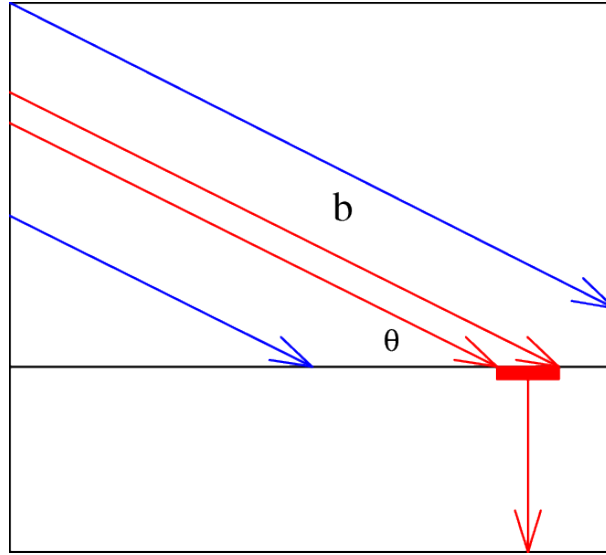
Figure 1: Sketch of the test configuration, showing fieldlines in direction **b** and the boundary between anisotropic conductor and perfect insulator.

In Figure 1, $T = T_0 > 0$ over the interval on the left hand boundary that is connected by field in direction **b** with the thick red line, elsewhere on the blue fieldlines, $T = 0$. The red region lies on a black line which denotes the boundary between anisotropic conductor and perfect insulator. The exact steady-state solution has $T = constant$ along fieldlines, but numerical diffusion will result in non-zero T in the region of blue fieldlines. The relative size of this numerical diffusion must be estimated as a function of incidence angle θ, where interest attaches to small $\theta \leq 2^o$.

3.1.2 Intermediate Case

To test curvature effects the whole 2-D domain of Figure 1 could be distorted by conformal mapping (which preserves angles).

3.1.3 Realistic Case

This needs to be 3-D and involve JET divertor tile descriptions derived from the output of the CAD design tool, together with information describing the magnetic field as a function of position, which will be supplied. The magnetic equilibrium may be supplied analytically after Solovev, but the usual input is as an .eqdsk file. The EQDSK G format is a "non-standard" standard for solutions $\psi(R, Z), p(\psi), I(\psi)$ of the Grad-Shafranov equation, where ψ is the magnetic flux and (R, Z) are cylindrical coordinates in planes normal to the toroidal direction. The functions p and I give the variation of the pressure and toroidal field respectively. The basic standard for EQDSK G may be found at: `https://fusion.gat.com/theory/Efitgeqdsk` (which may be password-protected) or else at `https://w3.pppl.gov/ntcc/TORAY/G_EQDSK.pdf` The flux $\psi(R, Z)$ is sampled at uniformly spaced points on a direct product grid, for which the .eqdsk header defines the mesh-size,

as well as other useful information, such as the flux on axis and at boundary. Unfortunately the strict EQDSK G standard uses a Fortran format that does not require spaces between samples, hence there are many variants for languages that cannot handle this situation, that have introduced other features such as mistakes in field helicity, factors of 2π in the flux, etc. Routines that calculate magnetic field $\mathbf{B}$ using cubic spline interpolation could be made available. It would be desirable for the output of System 2-2 to be used.

3.1.4 Extended Case

An extended test would allow for heat transfer in the solid surface sketched at bottom of Figure 1, taking say thermal diffusivity for Tungsten $\kappa \approx 3 \times 10^{-5}\,\mathrm{m}^2\,\mathbf{s}^{-1}$.
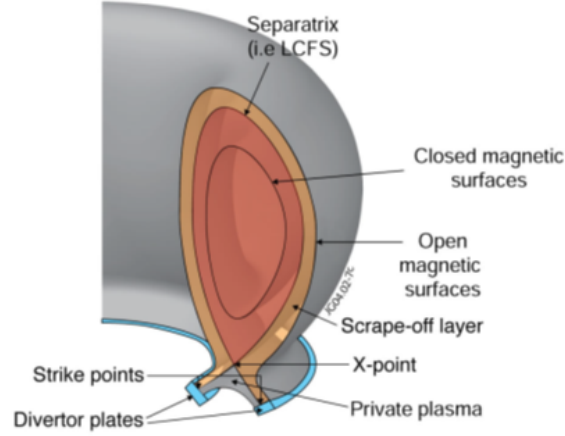
Figure 2: Sketch of the test configuration, showing tokamak cross-section and the boundary of the Last Closed Flux Surface (LCFS).

4 System 2-2: 2-D elliptic solver in complex geometry

The geometry will be representative of a tokamak cross-section, possibly omitting the region containing the central hot plasma, so that topologically it will be at most as complex as an annulus (one-hole). Figure 2 provides an example. The Last Closed Flux Surface (LCFS) may be parameterised by arc-length in the cross-sectional plane of projection.

The elliptic equations to be considered now follow.

4.1 Simplified Grad-Shafranov equation

This elliptic equation is a simplified version of the Grad-Shafranov equation, see [12]

$$R^2 \nabla \cdot \frac{1}{R^2} \nabla \psi = -2\mu_0 R j_\phi \tag{68}$$

where ψ is the poloidal magnetic flux and (R, Z) are cylindrical coordinates in planes normal to the toroidal direction ϕ, with the toroidal current

$$j_\phi = R \frac{dp(\psi)}{d\psi} + \frac{I}{\mu_0 R} \frac{dI(\psi)}{d\psi} + j_{ext}(R, Z) \tag{69}$$

The functions p and I give the variation as functions of ψ of the pressure and toroidal field respectively, and $j_{ext}(R, Z)$ may be produced in several ways, of which the commonest is by poloidal field circuits, ie. localised current sources in cross-section. Note that the operator in Equation (68) simplifies to

$$\frac{\partial^2}{\partial R^2} - \frac{1}{R} \frac{\partial}{\partial R} + \frac{\partial^2}{\partial Z^2} \tag{70}$$

which implies that mathematically, ψ satisfies a steady-state 2-D advection-diffusion equation corresponding to unit diffusivity in the flow $u_R = 1/R$.

16

To provide the simple test case, take $j_\phi = j_{ext}$ only with localised current sources. The boundary conditions are $\psi = 0$ on the LCFS and $\psi \propto 1/\sqrt{(R^2 + Z^2)}$ as R, $Z \to \infty$.

Note that the Grad-Shafranov equation has been solved using spectral elements by others, eg. Sovinec [3].

4.2 Simplified non-Boussinesq vorticity equation

A simplified version of the non-Boussinesq vorticity equation to be solved for the scalar field $\Phi(R, Z)$ in cylindrical polar coordinates (R, Z) is

$$\nabla_\perp \cdot \left(\frac{1}{B^2} \nabla_\perp \Phi \right) = n \tag{71}$$

where $B = |\mathbf{B}|$ is the amplitude of the imposed magnetic field, density n acts as a source term, and the elliptic is to be solved for Φ, subject to boundary conditions $\Phi = 0$. The operator $\nabla_\perp$, ignoring the components of magnetic field directed within the (R, Z) plane, reduces to the usual gradient ∇ in cylindrical polars of axisymmetric fields, hence mathematically Equation (71) is equivalent to Equation (68).

n will be set so that $n = n_0(s_i)$ on the boundaries, where arc-length s_i parameterises the inner boundary if $i = 1$ and the outer if $i = 2$. n and $|B|$ will be specified functions of (R, Z) that capture features of the number density n distribution and magnetic field intensity distribution expected in a tokamak, Ideally $|B|$ would represent a solution of the Grad-Shafranov equation from Section 4.1.

5 System 2-3: 1-D fluid solver with simplified physics but with UQ and realistic boundary conditions

5.1 Plasma Equations

Starting from the two-fluid model of Braginskii [8], a set of equations resembling those of classical (compressible) hydrodynamics may be derived by summing Braginskii's equations for number density, momentum and energy [13]. Using the standard notation of Section B, introducing $T_d = T_i + T_e$, neglecting the stress tensor terms (implicitly setting $\delta p_i = 0$), and assuming B is independent of time, the resulting system is

$$\frac{\partial}{\partial t}\left(\frac{N}{B}\right) + \frac{\partial}{\partial s_\parallel}\left(\frac{NU}{B}\right) = \frac{S^n}{B} \tag{72}$$

$$\frac{\partial}{\partial t}\left(\frac{NU}{B}\right) + \frac{\partial}{\partial s_\parallel}\left(\frac{NU^2}{B}\right) = -\frac{1}{m_i B}\frac{\partial}{\partial s_\parallel}(p_i + p_e) + \frac{S^u}{m_i B} \tag{73}$$

$$\frac{\partial}{\partial t}\left(\frac{3}{2}\left(\frac{NK_{AM}T_d}{B}\right) + \frac{1}{2}\left(\frac{NU^2}{B}\right)\right) +$$

$$\frac{\partial}{\partial s_\parallel}\left(\frac{5}{2}\left(\frac{NUK_{AM}T_d}{B}\right) + \frac{1}{2}\left(\frac{NU^3}{B}\right)\right) = -\frac{1}{m_i B}\frac{\partial}{\partial s_\parallel}(q_{i\parallel} + q_{e\parallel}) + \frac{(S_i^{\mathcal{E}} + S_e^{\mathcal{E}})}{m_i B} \tag{74}$$

where $s_\parallel$ is distance along the fieldline, and all variables retain their physical dimension. (Some variables from [13] have been promoted to capitals to indicate that they retain their physical dimensions.) The constant K_{AM} is such that

$$K_{AM} = \frac{k_B}{m_i} \text{ or } K_{AM} = \frac{|e|}{m_i} = \frac{|e|}{Am_u} \tag{75}$$

where k_B is Boltzmann's constant and $|e|$ is the unit of charge, depending whether T is measured in Kelvin or eV, A is atomic mass of the ion and m_u is the atomic mass unit.

Note that in adding Eqs.(3) and (4) of [13], equipartition and collision terms cancel to give Equation (74). The perfect gas equation of state will be assumed, so that

$$\frac{p_i + p_e}{m_i} = NK_{AM}T \tag{76}$$

The thermal conduction fluxes are

$$\frac{q_{\alpha\parallel}}{m_i} = -\kappa_\parallel^\alpha \frac{\partial K_{AM}T_\alpha}{\partial s_\parallel}, \quad \alpha = e,\ i \tag{77}$$

where the $\kappa_\parallel^\alpha$ take Braginskii values, see Section 2, thus for usual situation in which the electron conduction dominates

$$\frac{q_{i\parallel} + q_{e\parallel}}{m_i} = \kappa_\parallel^e \frac{\partial K_{AM}T_e}{\partial s_\parallel} \tag{78}$$

and T_e has be expressed in terms of T_d, eg. $T_e = T_d/2$ or $T_e = (1 - \tau^2)T_d$ in terms of an arbitrary $0 < \tau < 1$ to be introduced later. To give an easier test problem, the conduction term may be accounted for by augmenting the advective energy flux, $5/2 \rightarrow g$.

The boundary conditions are that $|U| = |M_s|C_S$ at $s = 0, 1$ where the sound speed

$$C_S = \sqrt{K_{AM}T_d} \tag{79}$$

and $|M_s|$ is the Mach number, since M_s will be allowed to take either sign. Normally $|M_s| = 1$ so that $M_0 = -1$ and M_1=1 where the subscript corresponds to value of s. The combined energy flux at each boundary has

$$|Q_\parallel| = \frac{1}{2}C_S N(\delta_e m_i K_{AM}T_e + \delta_i m_i K_{AM}T_i) \approx \frac{1}{2}m_i C_S N \delta m_i K_{AM}T_d \tag{80}$$

if $\delta \approx \delta_e \approx \delta_i$. For definiteness, $\delta = \frac{1}{2}(\delta_e + \delta_i)$ will be assumed. Values of δ_α from the literature imply $\delta = 4.25$. The energy flux factor g is chosen such that the easier model has the same energy flux.

For mathematical analysis, it is convenient to replace the source terms in Equations(72)– (74) with equivalent fluxes, however this is unnecessary for computational purposes. The forms the sources take are discussed below in Section 5.2.

5.2   Explicit Sources

The above work considers the case where the source terms are regarded as given, however it is worth describing the form of the additional sources that may be at least locally important. From ref [13], the plasma sources are given by (with the convention that suffix 'n' denotes neutral species)

$$S^n = N_n N \langle \sigma v \rangle_{ION} - N^2 \langle \sigma v \rangle_{REC} + S^n_\perp \tag{81}$$

$$\frac{S^u}{m_i} = N_n N \langle \sigma v \rangle_{ION} U_n - N^2 \langle \sigma v \rangle_{REC} U + N_n N (U_n - U) \langle \sigma v \rangle_{CX} \tag{82}$$

$$S^{\mathcal{E}} = S^{\mathcal{E}}_i + S^{\mathcal{E}}_e \tag{83}$$

$$= N_n N \langle \sigma v \rangle_{ION} (\frac{3}{2}kT_n + \frac{1}{2}m_n U_n^2 - kI_H) \tag{84}$$

$$- N^2 \langle \sigma v \rangle_{REC} (\frac{3}{2}kT_i + \frac{1}{2}m_i U^2)$$

$$+ N_n N \langle \sigma v \rangle_{CX} \left(\frac{3}{2}k(T_n - T_i) + \frac{1}{2}m_n(U_n^2 - U^2) \right)$$

$$- N_n N k Q_H + S^{\mathcal{E}}_{\perp i} + S^{\mathcal{E}}_{\perp e}$$

Here suffix $\perp$ denotes the effectively given source terms arising from cross-field contributions, suffices ION, REC and CX denote respectively reaction rates $\langle \sigma v \rangle$ for ionisation, recombination and charge-exchange, I_H is the Hydrogen reionisation potential, and Q_H is the cooling rate due to excitation.

Since the sources appear in the analysis primarily as integrals starting at $s = 0$, study of Equations(81)– (83) concentrates on this region, where plasma velocity $U < 0$ and neutral velocity $U_n > 0$ with the two having approximately the same magnitude. There, Equation (81) has only one negative term, due to recombination, but from the cross-section data in ref [13], this could

dominate only below $2\,$eV. All terms in Equation (82) are positive near $s = 0$ as the two velocities reinforce. Equation (83) contains two terms which are always negative and an ionisation term which is also negative below $I_H/2 \approx 7\,$eV, thus for example, the cross-field source terms $S_{\perp i,e}$ must be positive for $S^{\mathcal{E}} > 0$ in steady state.

The sources of neutrals may be deduced from the ionisation and charge-exchange terms in Equations(81)– (83), viz.

$$S_n^n = -N_n N \langle \sigma v \rangle_{ION} + S_{\perp n}^n \tag{85}$$

$$\frac{S_n^u}{m_n} = -N_n N \langle \sigma v \rangle_{ION} U_n - N_n N (U_n - U) \langle \sigma v \rangle_{CX} + S_{\perp n}^u \tag{86}$$

$$S_n^{\mathcal{E}} = -N_n N \langle \sigma v \rangle_{ION} (\frac{3}{2} k T_n + \frac{1}{2} m_n U_n^2 - k I_H) \tag{87}$$

$$- \quad N_n \langle \sigma v \rangle_{CX} \left(\frac{3}{2} k (T_n - T_i) + \frac{1}{2} m_n (U_n^2 - U^2) \right) \tag{88}$$

$$+ \quad S_{\perp n}^{\mathcal{E}} \tag{89}$$

The $S_{\perp n}$ terms are hard to quantify, but if these are neglected, it is clear that $S_n^n < 0$ and $S_n^u < 0$ is the obverse of the positive plasma sources. Similarly it is likely that $S_n^{\mathcal{E}} < 0$ if $S^{\mathcal{E}} > 0$

5.3 Dimensionless Coupled System

Treating Dimensionality It is assumed that the single spatial dimension of the problem corresponds to the arc length distance along a fieldline. There is the subtlety that number density should then be per metre, ie. m^{-1}, which is avoided by supposing that the volume considered has a cross-section of one square metre $1\,m^2$.

To proceed, it is helpful to make the preceding system of equations dimensionless. For the case of a fieldline connecting two walls at $s_\parallel = \pm L$, suppose dimensionless s, $0 \le s \le 1$) parameterises distance

$$s_\parallel = L(2s - 1) \tag{90}$$

It is therefore helpful to make fieldline length dimensionless in terms of the distance (assumed constant)

$$L_s = \frac{ds_\parallel}{ds} \tag{91}$$

and so $L_s = 2L$. Number density N should in any event be brought to a more manageable size, anticipating use of shorter word representations at Exascale, by dividing by a large (dimensionless) number N_{ref}. In addition, dependence of scalings on atom-specific properties should be avoided, leading to the introduction of

$$K_M = \frac{|e|}{m_u} \quad \text{so} \quad K_{AM} = \frac{|K_{AM}|}{A}, \quad K_M \approx 10^8 Ckg^{-1} \tag{92}$$

More precisely $K_M \approx 9.649 \times 10^7 \, Ckg^{-1}$.

Hence the variables should be made dimensionless by scaling N with respect to $N_0 \rightarrow N_{s,ref} = N_{ref}/L_s^D$, U with respect to $U_s = L_s/t_s$, T_d (in eV) with respect to $T_s = U_s^2/K_M = (L_s/t_s)^2/K_M$,

and B with respect to B_s. (D is the spatial dimensionality of the system, all notation follows the table in Section B.) Setting

$$N = \frac{nN_{ref}}{L_s^D}, \quad U = u\frac{L_s}{t_s}, \quad T_d = T\frac{L_s^2}{t_s^2 K_M} \tag{93}$$

then it is convenient to proceed by dividing the equations for particle density, momentum and energy by N_{ref} and then multiplying the equations for particle density Equation (72), momentum/ion Equation (73) and energy/ion Equation (74) by respectively

$$L_s^D t_s, \quad L_s^D t_s/U_s = \mathchar'26L_s^{D-1} t_s^2 \text{ and } L_s^D t_s/U_s^2 = \mathchar'26L_s^{D-2} t_s^3 \tag{94}$$

Note in particular that though it is tempting to include a factor 2 in the multiplicative scaling of the energy equation, this has to be seen as a hazard for coding purposes. Even more dangerous is the inclusion of purely numerical factors in the scaling of individual variables, and the use of N_{ref} has to be regarded as exceptional. The demands of numerics are in contrast with the need of analytic work to eliminate as many inessential factors as possible.

5.3.1 Choice (of Values) of Units

For code expected to be used for a wide range of plasma species and physical models, it is important to make the choice of units as neutral as possible. Thus it should not be based on the assumption of outflows at the sound speed of a particular species, as other outflow speeds might be found in the multispecies case. The parameter K_M has been introduced so that its value is set in terms of absolute physical constants, so that all physical scalings may be set by choice of L_s and t_s.

In the current context of a fieldline following system of equations, $L_d = 10\,\text{m}$ is a plausible length of fieldline and the timescale might be constrained by plasma sound speeds of order $10^5\,ms^{-1}$, ie. so that $t_s = L_s/10^5\,ms^{-1} = 10^{-4}\,s$. For the numerical scaling quantity, $N_{ref} = 10^{18}$ is memorable for an Exascale project, although perhaps one to two orders of magnitude larger than might otherwise have been chosen, and $N_{s,ref} = 10^{15}\,m^{-3}$ if $D = 3$ and $L_s = 10\,\text{m}$ is a little too small. Characteristic temperature T_s evaluates to $10^{10}/(|e|/m_u) \approx 100\,eV$. To treat the electric field, U_s^2/K_M may also be regarded as the scaling for the electric potential expressed as voltage, so that a characteristic electric field is

$$E_s = \frac{L_s}{t_s^2 K_M} \approx 10\,Vm^{-1} \tag{95}$$

implying a characteristic magnetic field of

$$B_s = \frac{1}{t_s K_M} \approx 10^{-4}\,T \tag{96}$$

which is unfortunately rather small.

The further point is that the code should be written so that N_{ref}, L_s and t_s are parameters that could be set differently depending on context.

5.3.2 Boundary Conditions and Constraints

Suppose the sources are symmetrically disposed about $s_\parallel = 0$ such that $n(s) = n(1-s)$, $u(s) = -u(1-s)$ and $T(s) = T(1-s)$. Note that sheath boundaries will be plasma outflows implying $u(0) < 0$. The boundary conditions on (dimensionless) u are in general specified in terms of the (signed) Mach number

$$u(0) = M_0 \sqrt{T(0)/A}, \quad u(1) = M_1 \sqrt{T(0)/A} \quad (M_0 = -M_1) \tag{97}$$

and the dimensionless outward energy flux (not doubled) at the boundaries $s = 0, 1$ satisfies

$$|q(s)| = \delta n(s) T(s) u(s) \tag{98}$$

Let n_0, u_0 and T_0 denote the dimensionless values of N, $|U|$ and T respectively at $s = 0$. Thus the boundary conditions on the symmetric plasma are completely specified by setting field values at $s = 0$ of

$$n = n_0 \tag{99}$$
$$u = -u_0 = M_0 \sqrt{T_0/A} \tag{100}$$
$$T = T_0 \tag{101}$$

when a steady solution is possible in the absence of neutral source terms only if it is arranged so that the rest of the sources satisfy

$$\int{}' s^n ds' = 2u_0 n_0 \tag{102}$$

$$\int{}' s^u ds' = 0 \tag{103}$$

$$\int{}' s^{\mathcal{E}} ds' = 2\delta n_0 T_0 u_0 \approx (g+1) n_0 T_0 u_0 \tag{104}$$

Symmetry imply that constraint Equation (103) is automatically zero, since s^u must be antisymmetric about $s = 1/2$. There is a further relation to be satisfied at $s = 1/2$, since if u vanishes there, then

$$n \frac{du}{ds} = s^n \tag{105}$$

$$g n T \frac{du}{ds} = s^{\mathcal{E}} \tag{106}$$

implying on division that

$$g T(\frac{1}{2}) = \frac{s^{\mathcal{E}}}{s^n} \tag{107}$$

Note that if the sources s^n, s^u and $s^{\mathcal{E}}$ vanish at the boundaries then steady-state has the additional constraint of boundary conditions of zero gradient (Neumann conditions). However, this will not generally be true since the more realistic representation of the sources in terms of neutral density typically does not vanish.

Working within the flux-tube geometry, the equations for neutral transport take the same form as those used for plasma above, however the boundary conditions are different. In dimensionless units, they become at $s = 0$, supposing that $\mathsf{T}(0) = \tau^2 T_0$ and masses $m_n = m_i$,

$$\mathsf{u} = -\tau u_0 \frac{\mathsf{M}_0}{M_0} \tag{108}$$

$$\mathsf{nu} = -R_p nu|_0 \quad \rightarrow \mathsf{n}_0 = -R_p \frac{n_0}{\tau} \frac{\mathsf{M}_0}{M_0} \tag{109}$$

$$\mathsf{T} = \tau^2 T_0 \tag{110}$$

where n, u and T are neutral density, velocity and temperature made dimensionless using the same units as the corresponding plasma quantities, M_0 is the signed Mach number for the neutrals, and R_p is the recycling coefficient. Note that the neutral velocity at the boundary is inward to the plasma, ie. opposite to the plasma flow, usage of a sans-serif font to denote dimensionless neutral species quantities, and that n does not include a factor of $\tilde{b} = B/B_s$, as the neutral flux is not constrained by the flux tube.

5.3.3 Dimensionless Coupled System

A system explicitly modelling the coupling between plasma and neutrals may be derived by making non-dimensionless the sources set out in Section 5.2, ignoring recombination, and assuming same species $m_n = m_i$, unit-free $\mathsf{T} = \tau^2 T_0$ (neutral temperature taken equal to ion temperature, ie. as a fraction τ^2 of $T_d = T_e + T_i$ at s=0), giving 5 equations for the evolution of plasma density, velocity, total temperature, neutral density and neutral velocity:

$$\epsilon_r \frac{\partial}{\partial t} n + \frac{\partial}{\partial s}(nu) = \sigma_I n\mathsf{n} + s^n \tag{111}$$

$$\epsilon_r \frac{\partial}{\partial t}(nu) + \frac{\partial}{\partial s}(nu^2 + nT) = \sigma_I n\mathsf{n}\mathsf{u} + \sigma_C n\mathsf{n}(\mathsf{u} - u) + s^u \tag{112}$$

$$\epsilon_r \frac{\partial}{\partial t}\left(\frac{(g-2)}{2}nT + \frac{1}{2}nu^2)\right) +$$

$$\frac{\partial}{\partial s}\left(\frac{g}{2}nuT + \frac{1}{2}nu^3\right) = \sigma_I n\mathsf{n}(\frac{3}{2}[\tau^2\mathsf{T} - T_H] + \frac{1}{2}\mathsf{u}^2) + \sigma_C n\mathsf{n}(\frac{1}{2}\mathsf{u}^2 - \frac{1}{2}u^2)$$

$$- \frac{\sigma_E}{A}n\mathsf{n} + \frac{s^{\mathcal{E}}}{A} \tag{113}$$

$$\epsilon_r \frac{\partial}{\partial t}\mathsf{n} + \frac{\partial}{\partial s}(\mathsf{nu}) = -\sigma_I n\mathsf{n} + s_n^n \tag{114}$$

$$\epsilon_r \frac{\partial}{\partial t}(\mathsf{nu}) + \frac{\partial}{\partial s}(\mathsf{nu}^2 + \mathsf{n}\tau^2\mathsf{T}) = -\sigma_I n\mathsf{n}\mathsf{u} - \sigma_C n\mathsf{n}(\mathsf{u} - u) + s_n^u \tag{115}$$

where $\epsilon_r = t_s/t_0$ with t_0 a characteristic evolutionary timescale. All dimensionless temperatures should be divided by the atomic number A of the species if it is not unity ie. $T \rightarrow T/A$. The reaction

rates are made dimensionless by division by $U_s/(L_s N_{s,ref})(= 10^{5-1+3-18} = 10^{-11})\,m^3 s^{-1}$ so that

$$\sigma_I = \frac{\langle \sigma v \rangle_{ION}}{L_s^D/(t_s N_{ref})} \tag{116}$$

$$\sigma_C = \frac{\langle \sigma v \rangle_{CX}}{L_s^D/(t_s N_{ref})} \tag{117}$$

$$\sigma_E = \frac{Q_H}{T_s L_s^D/(t_s N_{ref})} = \frac{Q_H}{L_s^{D+2}/(t_s^2 N_{ref} K_M)} \tag{118}$$

$$T_H = \frac{I_H}{3T_s} \simeq 4.5/T_s \text{(in eV)} \tag{119}$$

where I_H and Q_H are as defined in ref [13]. The source terms S^n, S^u/m_i and $S^{\mathcal{E}}$ are made dimensionless by multiplication by $L_s^D t_s$, $L_s^{(D-1)} t_s$ and $L_s^{(D-2)} t_s/m_u$ respectively for Equation (72) Equation (73) and Equation (74). Spatially variable B is accounted for by identifying $n \to n/\tilde{b}$, $s^{n,u,\mathcal{E}} \to s^{n,u,\mathcal{E}}/\tilde{b}$, and dividing the term $\frac{\partial}{\partial s}(nT)$ in Equation (112) by $\tilde{b}$ (or by taking $\frac{\partial}{\partial s}(\ln \tilde{b})$ to be negligible).

It is of interest to allow a stochastic ('turbulent') contribution to the terms $s^{n,u,\mathcal{E}}$.

5.3.4 Symmetry and Constraints

As for the single plasma fluid case, provided the sources have the correct symmetries about the domain mid-point (symmetric for density and energy, antisymmetric for momentum), then the coupled system also has a solution with symmetries corresponding to the source terms, ie. density and temperature are symmetric and the flow antisymmetric.

In the steady state, there is the constraint that summed flux of neutral and plasma mass at boundary balances integrated source:

$$[nu + \mathsf{n}\mathsf{u}]_0^1 = \int_0^1 (s^n + s_n^n) ds' \tag{120}$$

whereas source anti-symmetry automatically ensures momentum conservation.

$$\left[nu^2 + nT + \mathsf{n}\mathsf{u}^2 + \mathsf{n}\mathsf{T} \right]_0^1 = 0 \tag{121}$$

5.4 Neutrals as 2-D or 3-D fluid

The above Equations(114) and (115) are a reduction to 1-D of the system

$$\epsilon_r \frac{\partial}{\partial t}\mathsf{n} + \nabla \cdot (\mathsf{n}\mathsf{u}) = -\sigma_I n \mathsf{n} + s_n^n \tag{122}$$

$$\epsilon_r \frac{\partial}{\partial t}(\mathsf{n}\mathsf{u}) + \nabla \cdot (\mathsf{n}\mathsf{u}\mathsf{u}) + \nabla \mathsf{n}\mathsf{T} = -\sigma_I n \mathsf{n}\mathsf{u} - \sigma_C n \mathsf{n}(\mathsf{u} - \mathbf{u}) + s_n^u \tag{123}$$

24

6 System 2-4: Spatially 1-D plasma model incorporating velocity space effects

The following simple model is after Taitano et al [14, 15]

$$
\begin{aligned}
\frac{\partial f_e}{\partial t} + v_{ex}\frac{\partial f_e}{\partial x} + \frac{q_e}{m_e}\mathbf{E}\cdot\frac{\partial f_e}{\partial \mathbf{v}} &= 0 \\
\frac{\partial f_i}{\partial t} + v_{ix}\frac{\partial f_i}{\partial x} + \frac{q_i}{m_i}\mathbf{E}\cdot\frac{\partial f_i}{\partial \mathbf{v}} &= 0 \\
\epsilon_0\frac{\partial \mathbf{E}}{\partial t} + \sum_\alpha q_\alpha n\mathbf{u}_\alpha - \overline{\sum_\alpha q_\alpha n\mathbf{u}_\alpha} &= 0
\end{aligned}
\tag{124}
$$

Equations 124 are the electron and ion Vlasov equations and Ampere's equation respectively. The quantities m_e, m_i, f_e, f_i, $\mathbf{v}_e$, $\mathbf{v}_i$, q_e, q_i, $\mathbf{E}$, ϵ_0, and $n\mathbf{u}_\alpha$ are the electron and ion masses, electron and ion distribution functions, electron and ion velocities, electron and ion charges, the electric field, permeability constant of vacuum, and the momentum of species $\alpha = i, e$, respectively. Note that Equation (124)represents a generalisation of the system in ref [14], where for vector quantities, the x-component is always implied, in the usual notation the original system is $1d1v$ rather than $1d3v$ as above, where particles move according to

$$
\begin{aligned}
\frac{dx}{dt} &= v_{\alpha x} \\
\frac{d\mathbf{v}_\alpha}{dt} &= \frac{q_\alpha}{m_\alpha}\mathbf{E}
\end{aligned}
\tag{125}
$$

(Motion in (y, z) is neglected, the 3-D electromagnetic version of Equation (125) appears in Section 10).

The $\overline{\sum\cdot}$ term denotes for example a spatially averaged summed quantity and is included to enforce Galilean invariance. The solutions f_e and f_i of the Vlasov equations are functions of space variable x, velocity $\mathbf{v}$, and time. Ampere's equation is solved for the self-consistent electric field $\mathbf{E}$, which is a function of space variable x and time.

The boundary conditions used are periodicity in x, and zero at infinity in $|\mathbf{v}|$. Initial conditions which might be used for the distribution functions are from ref [14],

$$
\begin{aligned}
f_0(x, \mathbf{v}, \mathbf{u}_0, T_0) &= \frac{n_0(x)}{\sqrt{2\pi kT_0/m}}\exp\left(-\frac{m(\mathbf{v}-\mathbf{u}_0)^2}{2kT_0}\right) \\
n_0(x) = n(t = 0, x) &= 1 + \alpha_n\cos(k_w x)
\end{aligned}
\tag{126}
$$

where n_0, $\mathbf{u}_0$ and T_0 are the initial number density, initial fluid velocity and initial temperature respectively. The parameter α_n is the perturbation amplitude, k_w is its wave vector, and m is the species mass. It follows that the (scaled) momentum is given formally as

$$
n\mathbf{u}_\alpha(x) = \int \mathbf{v}f_\alpha(x, \mathbf{v}, t)d\mathbf{v}
\tag{127}
$$

where f_α is the distribution function for species α at time t. (In practice the integral would be replaced by a sum over particles.)

Note that periodic boundary conditions are of limited value in practice, and attention should be given to minimal modifications of the above problem where there is

1. a flux of momentum across the domain (inflow and outflow boundary conditions)

2. reflection of particles at the boundaries

3. a source of plasma within the domain, and outflow boundaries

4. and where the spatial dimension corresponds to arc length s along a fieldline (implies n replaced by $n/|\mathbf{B}|$, cf. Section 5.1).

7 System 2-5: Spatially 1-D multispecies plasma model

7.1 Fluid model

For a multispecies plasma, there is a system of Boltzmann equations to be solved, one for each species, each of form in 3 spatial dimensions

$$\mathcal{L}_7 f_\alpha = \sum_\beta Q(f_\alpha, f_\beta) + S_\alpha \tag{128}$$

where $\mathcal{L}_7$ is the 7-D Lie derivative (space, velocity-space and time make up the $3 + 3 + 1 = 7$ dimensions, α, β are species labels and Q is the Boltzmann collision operator. The multispecies equations are derived following Grad [16, §6] by substituting in Equation (128)

$$f_\alpha = \exp(-\lambda H_\alpha)\mathcal{F}_\alpha(x, \mathbf{v}, t) \tag{129}$$

where the flow of the Lie derivative is given by the Hamiltonian H_α and $\mathcal{F}_\alpha$ is a functional of moments of f_α, to include (dropping the suffix on f)

$$n = \int f d\mathbf{v}, \ \ \mathbf{u}_0 = \int f\mathbf{v}d\mathbf{v}, \ \ T = \int fv^2/2d\mathbf{v} \tag{130}$$

The resulting system is linearised and solved by iteration to give the multispecies plasma fluid equations in Zhdanov [16, §6]. There are believed to be typographical errors in Zhdanov, so cross-checking is needed.

To see Grad's approach applied to classical fluids see for example [17, §8].

7.2 Coupling to particles

Other, less collisional species are to be treated as particles as in Section 6 and coupled via S_α. Mathematical forms for S_α will be guided by the emerging results from particles' method research.

8 System 2-6: Spatially 2-D plasma model incorporating velocity space effects

With reference to the Hermes web-site [18], the following 2-D time dependent model of plasma evolution may be derived, expressed using the agreed notation for plasma quantities, see Section B, note in particular that plasma 'vorticity' has dimensions of charge density.

$$p = \sum_\alpha n_\alpha k T_\alpha \tag{131}$$

$$\rho_m = \sum_\alpha A_\alpha m_u n_\alpha \tag{132}$$

$$c_s = \sqrt{\frac{p}{\rho_m}} \tag{133}$$

$$n_e = \Sigma_{\alpha \neq e} Z_\alpha n_\alpha = Z_i n_i \tag{134}$$

$$\frac{\partial n_e}{\partial t} = -\nabla \cdot (n_e \mathbf{v}_{E \times B}) + \nabla \cdot \frac{1}{|q_e|} \mathbf{j}_{sh} - \frac{n_e c_s}{L_\parallel} + S_e^n \tag{135}$$

$$\frac{\partial p_e}{\partial t} = -\nabla \cdot (p_e \mathbf{v}_{E \times B}) - \frac{\delta_e p_e c_s}{L_\parallel} + S_e^p + D_{fpe} \nabla \cdot (\kappa_{e\perp} n_e \nabla_\perp k T_e) \tag{136}$$

$$\frac{\partial p_i}{\partial t} = -\nabla \cdot (p_i \mathbf{v}_{E \times B}) - \frac{\delta_i p_i c_s}{L_\parallel} + S_i^p + D_{fpi} \nabla \cdot (\kappa_{i\perp} n_i \nabla_\perp k T_i) \tag{137}$$

$$\tag{138}$$

$$\frac{\partial \omega}{\partial t} = -\nabla \cdot (\omega \mathbf{v}_{E \times B}) + \nabla \cdot \left[(p_e + p_i) \nabla \times \frac{\mathbf{b}}{B} \right] + \nabla \cdot \mathbf{j}_{sh} + D_{fvs} \nabla \cdot \nu \nabla_\perp \omega \tag{139}$$

$$\nabla \cdot \left[\frac{m_i}{Z_i |q_e| B^2} \nabla_\perp \left(n_{ref} |q_e| \Phi + \frac{1}{Z_i} p_i \right) \right] = \omega \tag{140}$$

$$\nabla \cdot \mathbf{j}_{sh} = -\frac{|q_e| n_e c_s}{L_\parallel} \frac{|q_e| \Phi}{k T_{ref}} \tag{141}$$

$$\mathbf{v}_{E \times B} = \frac{\mathbf{B} \times \nabla \Phi}{B^2} \tag{142}$$

where it has been assumed that there is a single ion species i. (Cases with $Z_i \neq 1$ need checking, so the ion species has to be assumed Hydrogenic $Z_i = 1$ for now.) The sheath heat transmission coefficients are from Stangeby [19, §2.8] (who uses the notation 'γ_α')

$$\delta_e = 6.5, \quad \delta_i = 2.0 \tag{143}$$

Notes

1. The system is defined in two space dimensions, so both number n_e and charge (ω) density are defined per *square* metre, and pressure as force per unit *length*.

2. The dissipative terms with coefficients ν, $\kappa_{e\perp}$ and $\kappa_{i\perp}$ (Braginskii functional forms to be used from Section 2, enhanced if necessary by numerical multiplication factors D_{fpe}, D_{fpi}, D_{fvs}) have been added so that Hermes-3 simulations may be compared minimising complications due to sub-grid-scale effects.

3. Thanks to the use of equations for pressure instead of energy density ($\mathcal{E}_\alpha = \frac{3}{2}p_\alpha$, $\alpha = e, i$), Braginskii values correspond to $D_{fpe} = D_{fpi} = \frac{2}{3}$

4. Similarly the pressure sources are to be reduced $S_\alpha^p = \frac{2}{3}Q_\alpha$, $\alpha = e, i$.

5. The same expressions may be taken for the source terms as those listed in System 2-3 in Section 5

6. Successive simplifications for the pressure 'dissipation' replace

$$D_{fpe}\nabla \cdot (\kappa_{e\perp} n_e \nabla_\perp kT_e) \quad \rightarrow \quad D_{fpe}\nabla \cdot (\kappa_{e\perp} \nabla_\perp p_e) \tag{144}$$

$$D_{fpi}\nabla \cdot (\kappa_{i\perp} n_i \nabla_\perp kT_i) \quad \rightarrow \quad D_{fpi}\nabla \cdot (\kappa_{i\perp} \nabla_\perp p_i) \tag{145}$$

and then with adjusted numerical multiplication factors D_{fpe}^κ, D_{fpi}^κ:

$$D_{fpe}\nabla \cdot (\kappa_{e\perp} \nabla_\perp p_e) \quad \rightarrow \quad D_{fpe}^\kappa \nabla \cdot \nabla_\perp p_e \tag{146}$$

$$D_{fpi}\nabla \cdot (\kappa_{i\perp} \nabla_\perp p_i) \quad \rightarrow \quad D_{fpi}^\kappa \nabla \cdot \nabla_\perp p_i \tag{147}$$

$$\tag{148}$$

which are increasingly inaccurate but increasingly easier to implement.

8.1 Dimensionless units

NEPTUNE will *not* use dimensionless units because of the potential for confusion. However, the Hermes-3 models are expressed in dimensionless variables, and it is necessary to understand how this has been done. A prominent source of confusion is the introduction of purely numerical factors when transforming, for which there is one permissible exception namely, as in the Hermes-3 model, where the opportunity has been taken to introduce a factor N_{ref} to reduce number densities to more reasonable magnitudes. The key scalings are

1. time in units of $1/\omega_{ci}$,

2. length in units of $c_{s,ref}/\omega_{ci}$, where the speed satisfies $kT_{ref} = m_i c_{s,ref}^2$

3. electric potential in units of $kT_{ref}/|q_e|$

4. magnetic field in units of B_0 used to define $\omega_{ci} = Z_i|q_e|B_0/m_i$ (remembering $Z_i = 1$ in the model).

5. n_e, p_i, p_e, ω made dimensionless with respect to an additional factor of $N_{ref}\times$ the expected scalings of $(\omega_{ci}/c_{s,ref})^2$, $m_i\omega_{ci}^2$, $m_i\omega_{ci}^2$ and $|q_e| \cdot (\omega_{ci}/c_{s,ref})^2$ respectively.

6. consequently dimensional source terms have to be scaled (divided) by $N_{ref}\omega_{ci}$Scale where Scale is the appropriate factor for the equation from the preceding list.

(It is suggested that in keeping with the application to the Exascale, the pure number $N_{ref} = 10^{18}$.) In the Hermes-3 equations, variable 'c_s' becomes the Mach number, variable 'e'=-1, $L_\parallel$ is in units of $c_{s,ref}/\omega_{ci}$. (Quoted variables indicate that they are not NEPTUNE approved symbols.) The NEPTUNE website has a section on "Physical properties of the edge plasma" which gives representative values for the units employed above.

8.2 Boundary conditions

Boundary conditions employed are typically Neumann or Dirichlet.

8.3 Initial conditions

Initial conditions rely on simple analytic responses to source terms that may be either of volume form meaning imposed contributions such as S_e^n above (representing eg. gas-puffing), or expressed as inflows, either from the hot central plasmas or due to recycling of plasma at the first wall. By default the source terms will each have a Maxwellian distribution. The presence of large, possibly dominant source terms implies a need to ramp up solutions. A two stage process is suggested, whereby first an analytic approximation S_{ana} to the expected source say S_α^n is specified, so that for $t < t_R$

$$S_\alpha^n(t) \approx S_{\mathrm{num}}^n = \frac{t}{t_R} S_{\mathrm{ana}} \tag{149}$$

thereafter introduce a hand-off function $w_H(t - t_R)$ falling linearly from 1 to 0 over a time t_H so that

$$S_{\mathrm{num}}^n = w_H S_{\mathrm{ana}} + (1 - w_H) S_\alpha^n \tag{150}$$

where mathematically

$$w_H(t') = 1 - t'/t_H, \ \ t' = t - t_R \tag{151}$$

8.4 Kinetic effects

A particle (PIC) model, see Section 9 may be used to compute models to represent the sheath instead of the terms in $\nabla \cdot \mathbf{j}_{sh}$ above.

As an alternative (or additional) means of including particle effects, the source terms S_e^n, S_α^p, $\alpha = e, i$ may be calculated by Monte-Carlo techniques, see Section 11 for treatment of particle interactions. (Necessary Monte-Carlo techniques for particle production and motion are described in Section 10.)

9 Systems 3: Kinetic models

The following generic transport equation [20, § 1] applies to all particle-based models for the time evolution of the density distribution function $f(x, \mathbf{v}, t)$

$$\frac{\partial f}{\partial t} + \mathbf{v} \cdot \frac{\partial f}{\partial \mathbf{x}} + \mathbf{a} \cdot \frac{\partial f}{\partial \mathbf{v}} = S_C(f) = \left(\frac{\partial f}{\partial t}\right)_C + S_{exp}(\mathbf{x}, \mathbf{v}, t) \tag{152}$$

where $\mathbf{a} = d^2\mathbf{x}/dt^2$ is the acceleration experienced by a particle at position $\mathbf{x}$ with velocity $\mathbf{v}$. This represents scalar advection in a 6-D space with an explicit source $S_{exp}(\mathbf{x}, \mathbf{v}, t)$ and a source due to other inter-particle interactions that is conventionally written $(\partial f/\partial t)_C$ when it is localised and usually depends linearly on f. Ultimately it will be necessary to solve a multi-species version of Equation (152) complete with appropriate source terms to represent the physics thought critical for modelling the tokamak edge.

Complete specification of the problem even for $S_C = 0$ and a single species of particle requires a force law such as that for particles of species α with charge q_α and mass m_α

$$\mathbf{F} = m_\alpha \frac{d^2\mathbf{x}}{dt^2} = q_\alpha (\mathbf{E} + \mathbf{v} \times \mathbf{B}) \tag{153}$$

and equations for the evolution of the electromagnetic fields $\mathbf{E}(\mathbf{x}, t)$ and $\mathbf{B}(\mathbf{x}, t)$ such as Maxwell's equations, neglecting displacement current. Inevitably choice of S_C is a function of lengthscale and timescale. On fast timescales in a strong electromagnetic field, the effect of collisions can be ignored (collective effects are felt through the electromagnetic field), when the Particle-in-Cell or PIC approach [21] is effective. Note that strictly local particle-particle interactions should be accounted for, but these are expected to have negligible effect in a plasma (although not in a gravitating system).

For neutral particles, when often $\mathbf{a} = \mathbf{0}$, interest attaches to S_C which for 2-particle interactions is often the Boltzmann operator for different species $Q(f_\alpha, f_\beta)$ where α, β are species labels.

9.1 Particle-in-Cell (PIC)

Although PIC codes are conceptually simple to implement, in practice there is often a problem with statistical effects, *aka* noise. Noise is generally found to be reduced when the scheme is momentum conserving, which is usually achieved [21, § 5-3-3] by use of (1) the same function in both charge assigment and interpolation of force onto particles, and (2) space-centred approximations to derivatives. In the NEPTUNE symbols, assignment of charge to nodes and force interpolation to particles, share a weighting function W, such that

$$\Delta \rho_c(\mathbf{x}_m) = \frac{q_\alpha}{V^e} W(\mathbf{x}_p - \mathbf{x}_m) \tag{154}$$

$$\mathbf{F}(\mathbf{x}_p) = = \Sigma_m q_\alpha W(\mathbf{x}_p - \mathbf{x}_m) \mathbf{E}(\mathbf{x}_m) \tag{155}$$

where $\mathbf{x}_p$ is the position of the particle, $\mathbf{x}_m$ is the location of a finite element node. For consistency with the Nektar++ basis

$$W(\mathbf{x}) = \phi_{e,\xi}(\mathbf{x}) \tag{156}$$

The fundamental import of (2) is that

$$\mathbf{E}(\mathbf{x}_m) = \Sigma'_m V^e G(\mathbf{x}_m, \mathbf{x}'_m) \rho_c(\mathbf{x}'_m) \tag{157}$$

where $G(\mathbf{x}_m, \mathbf{x}'_m) = -G(\mathbf{x}'_m, \mathbf{x}_m)$. The antisymmetry of G then ensures vanishing of the particle self-force and that the forces exerted by one particle on another are equal and opposite, since eg.

$$\mathbf{F}(\mathbf{x}_p) = q_\alpha^2 \Sigma_m \Sigma'_m W(\mathbf{x}_p - \mathbf{x}_m) V^e G(\mathbf{x}_m, \mathbf{x}'_m) W(\mathbf{x}_p - \mathbf{x}'_m) \tag{158}$$

Only the electrostatic field $\mathbf{E}$ is shown in Equation (154) but the above analysis holds more generally for the Lorentz force.

10 System 3-1: 2-D particle-based model of neutral gas and impurities with critical physics

The neutrals are represented as super-particles that travel ballistically after introduction and are lost when they strike the first wall. In this context, neutral particle may include photons. Super-particles have label p, weight w_p and sample the point $(\mathbf{x}_p, \mathbf{v}_p)$ in 6-D position and velocity space. At introduction, all particle quantities are defined by sampling from specified probability distributions.

10.1 Prerequisites

10.1.1 Parameters

It is necessary to have parameters describing initial and boundary conditions. There must be a means of tying boundary conditions to specific parts of the surface and volume geometry. See discussion of definitions of objects/classes for NEPTUNE in web pages.

10.1.2 Random number generator

It is generally important to test the properties of a random number generator to ensure there is an absence of bias, typically by producing histograms of the output and comparing with expected curves. If other routines are found to be unsuitable, a technique based on the 'Mersenne Twister' should give a satisfactory sequence of pseudo-random numbers.

For a range of applications where functions or distributions do not vary on very small scales, Quasi-Monte Carlo sampling [22] may be preferable to Monte Carlo. Note that although the place-name Monte-Carlo has a hyphen, the name of the mathematical technique does not by convention. For parallel computation, it will generally be best to compute a block of numbers at a time.

10.1.3 Sampling from a specified distribution

Generally   Textbooks such as Kalos and Whitlock [23] (notable for its treatment of radiation transport in §6) explain how to generate samples of a given distribution $f(x)$ from random numbers uniformly sampled on the unit interval. Suppose that ξ is such a random number, then the corresponding value of x is given by solution of

$$\xi = 1 - \int_0^x f(x')dx' \tag{159}$$

Equation (159) may be solved explicitly for x in many important cases

Gaussian distribution   This may be sampled using the Box-Muller method [23, §3.1]. Given two random numbers ξ_1 and ξ_2 uniformly sampled on the unit interval, then two samples of a Gaussian distribution $f(x) \propto \exp(-x^2/2)$ are given by

$$\sqrt{[-2(\ln(1-\xi_1))]}\cos 2\pi\xi_2 \tag{160}$$
$$\sqrt{[-2(\ln(1-\xi_2))]}\cos 2\pi\xi_1 \tag{161}$$

Knudsen cosine   Sample by accept-reject from the Knudsen cosine distribution below Equation (162) to launch particle trajectories.

Let f_{max} and s_{max} be the maximum of the distribution function in $[0, 6v_{th,i,Kn})$ and the associated speed, respectively where $v_{th,i,Kn} = \sqrt{2kT_{Kn}/m_i}$). Then provide pairs of random numbers $R_f \in [0, f_{max}]$ and $v_R \in [0, 6v_{th,i,Kn}]$ (and other components of velocity similarly sampled for the tangential components (but with a negative velocity ranges)). Keep the particle with normal speed v_R if $R_f < f_{n,Kn}(v_R)$.

10.2   Sources and sinks of neutrals

10.2.1   Knudsen distribution

As suggested in the TN-07 Neptune report by Parra, Barnes and Hardman [24] equations (5.9)-(5.13), the source of neutrals emitted from a wall can be described by the Knudsen cosine distribution

$$f_{n,Kn}\left(\boldsymbol{v}; \boldsymbol{n} \cdot \boldsymbol{v} > 0\right) = \frac{3}{4\pi}\left(\frac{m_i}{kT_{Kn}}\right)^2 \frac{\boldsymbol{n} \cdot \boldsymbol{v}}{|v|}\exp\left(-\frac{m_i v^2}{2kT_{Kn}}\right) \tag{162}$$

where $\boldsymbol{n}$ is the normal to the wall, the Knudsen distribution is used for outgoing neutrals for which $\boldsymbol{n} \cdot \boldsymbol{v} > 0$, and kT_{Kn} is a parameter that controls the temperature of the emitted neutral distribution. The Knudsen cosine distribution appears with a factor of a particle flux in Equation (5.9) of [24], so despite the "f" notation, it has different units to the other distributions f.

10.2.2 Volumetric distribution

As a starting point, the source of neutrals should be fixed in time and given a prescribed spatial distribution around the edge of the simulation domain. A point source, ie. delta function in space, would be a valid representation of a 'gas valve'. Volumetric sources consisting of eg. a Maxwellian at a given temperature) could be considered for testing purposes.

10.2.3 Recycling

This cannot be properly treated without coupling to a plasma model, hence is treated in Section 11.4.1.

10.2.4 Particle sink

An explicit volume pumping region, where neutrals are absorbed when they reach it. This might be specified by a set of finite element identifiers e.

10.3 Boundary condition for neutral particles

The particle simulation domain need not coincide with the simulation domain, since there may be finite elements where a species is treated as a fluid.

10.3.1 Perfect Absorption

Any particles that reach a domain boundary are deleted.

10.3.2 Reflection

These conditions are very useful for testing eg. energy conservation. Perfect specular reflection might be needed to handle symmetry. Supposing the unit surface normal is n, if the incident velocity is $\mathbf{v_p}$, then the reflected particle has velocity

$$\mathbf{v_p} = \mathbf{v_p} - 2(\mathbf{v_p}.n)n \tag{163}$$

10.3.3 Periodic boundaries

These conditions are very useful for testing purposes, and required for full or repeat sections of toroidal geometry. Particles simply leave one end of the domain and re-enter at the other. In the case of a rectilinear grid, periodic boundary conditions are easily applied by taking the modulus of the coordinate value with respect to the period length.
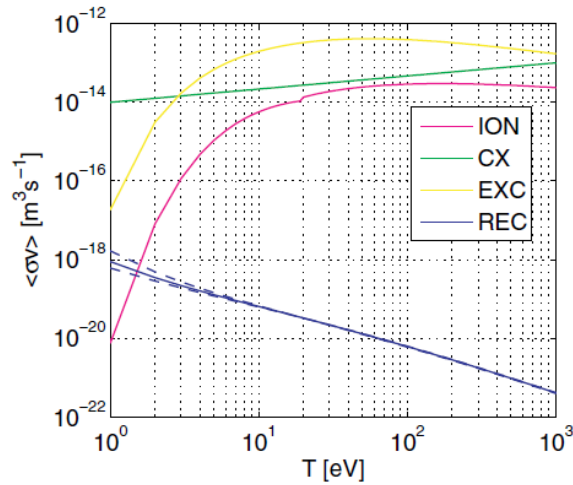
Figure 17. Collision rates used in the SOLF1D code. The recombination rate is displayed for densities $n = 1 \times 10^{18} \, \mathrm{m}^{-3}$, $n = 1 \times 10^{19} \, \mathrm{m}^{-3}$ and $n = 1 \times 10^{20} \, \mathrm{m}^{-3}$.

Figure 3: Extract from publication indicated in the text.

10.3.4 Imperfect reflection

These conditions are probably most appropriate for photons. This may be achieved by arranging that a fraction $(1 - R_p)$ of incident particles are absorbed. If the particles are allowed different weights, then simply reduce the weight w_p of each reflected particle by the particle recycling factor R_p and its energy consistent with recycling factor R_E. Sputtering is the ejection of surface atoms by impact of both energetic ions and neutrals. However, the rates of sputtering by energetic neutrals are relatively low below $100 \, \mathrm{eV}$ [10, § 9.7] and may be negelcted in an initial investigation.

11 System 3-3: Interaction with 2-D plasma model

11.1 Prerequisites

11.1.1 Cross-section data input

Cross-section data will be obtained from the ADAS library [25]. Cross-section data $\langle \sigma v \rangle$ averaged over a Maxwellian velocity distribution suitable for use by a fluid model of the plasma edge is shown in Figure 3, from Havlickova et al. [13]. The dominant relevant reactions affecting both neutrals and plasma in the graph are

$$\text{Ionisation (ION)} \quad e^- + H \quad \rightarrow \quad H^+ + e^- + e^- \tag{164}$$

$$\text{Charge-exchange (EXC)} \quad H + H^+ \quad \rightarrow \quad H^+ + H \tag{165}$$
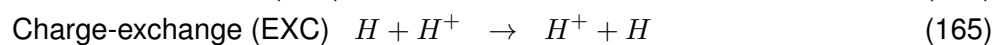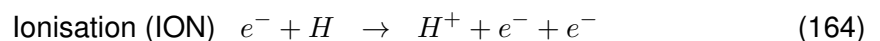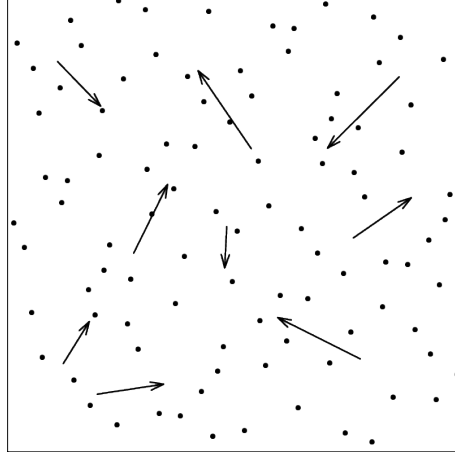
Figure 4: Configuration for ionisation. Neutrals, indicated by arrows, moving against a background of thermal electrons shown as dots.

11.2 Physical Models

11.2.1 Introductory model

Perhaps the simplest model to consider is that for ionisation of neutrals by electron impact. A simple model for ionisation can be written as:

$$\frac{\partial f_n}{\partial t} = \ldots - R_{ION} n_i f_n \tag{166}$$

$$\frac{\partial n_i}{\partial t} = \ldots + R_{ION} n_i n_n \tag{167}$$

where R_{ION} ($\langle \sigma v \rangle_{ION}$ elsewhere) is a constant ionisation rate, f_n is the distribution function for the neutrals, n_i and n_n are the ion and neutral densities. The quasineutrality assumption implies $n_e = n_i$. So the 'source term' in the plasma density equation is

$$S_{ION}(\mathbf{x}) \equiv R_{ION} n_i n_n = R_{ION} n_i \int d^3 v \, f_n(\boldsymbol{v}) \tag{168}$$

the integral in which converts, for number densities, into weighted counts of the number of particles within a given spatial volume about point $\mathbf{x}$.

The loss term in the neutral density equation is computed using Monte Carlo techniques, cf. Verboncouer [26], configuration sketched in Figure 4. The probability of ionisation of a particle at time t_n travelling with velocity $\mathbf{v}_p$ in the following interval of Δt is

$$\mathrm{p}_p(t_n) = 1 - \exp\left(-n_e \sigma_{ION} |\mathbf{v}_p| \Delta t\right) \tag{169}$$

where the cross-section for ionisation is σ_{ION}. Provided the background density n_e is approximately constant in space and time, and σ_{ION} variation with energy $\mathcal{E}$ is assumed to be negligible, taking for example

$$\nu_{\sigma max} = \max_{\mathbf{x}} \{n_t(\mathbf{x})\} \max_{\mathcal{E}} \{\sigma_T(\mathcal{E})|\mathbf{v}|\} \tag{170}$$

36

then for every particle, provided all particles have the same weight (ie. identical superparticles), approximately

$$p_p = p_T = 1 - \exp\left(-\nu_{\sigma max} t\right) \tag{171}$$

and the number of neutrals that undergo ionisation in volume ΔV is $p_T n_n \Delta V$. Such particles should be chosen at random from those in ΔV.

The Monte Carlo algorithm for selecting which neutrals turn into ions, is simple provided that particles are distributed at random throughout ΔV, viz. to obtain a random number ξ from the uniform distribution on the unit interval (ie. $0 < \xi < 1$) for each particle in turn and if at the qth $\xi < p_T$ then the qth particle is regarded as ionised at time t_n. If particles are each allowed a weight $w_p(t)$ which varies with time, then the weight of the neutral may simply be reduced to account for the ionisation

$$w_p(t_n + \Delta t) = p_p(t_n) w_p(t_n) \tag{172}$$

11.2.2 Detailed model

For sources in the fluid equations due to ionisation of neutrals by electrons, the formulae, cf. Equations(85)– (87) ([13, Eqs.(34)-(36)]) are

$$S_e^n = N_n N \langle \sigma v \rangle_{ION} \tag{173}$$

$$\frac{\mathbf{S}_n^{\mathbf{v}}}{m_n} = N_n N \langle \sigma v \rangle_{ION} \mathbf{v}_n \tag{174}$$

$$S_e^p = -\frac{2}{3} N_n N \langle \sigma v \rangle_{ION} k I_H \tag{175}$$

$$S_i^p = \frac{2}{3} N_n N \langle \sigma v \rangle_{ION} \left(\frac{3}{2} k T_n + \frac{1}{2} m_n \mathbf{v}_n^2\right) \tag{176}$$

Note that other effects due to charge-exchange and recombination may be deduced from the equations in Section 5.2. Monte Carlo calculation may then proceed using a total cross-section for all three interactions.

11.2.3 Simplified model

For an exploratory calculation with the Hermes-3 equations, the ionisation potential term is an unwelcome complication and the momentum term is assumed not to contribute to the evolution of the vorticity ω. Hence Equations(173)– (176) above become

$$S_e^n = N_n N \langle \sigma v \rangle_{ION} \tag{177}$$

$$\mathbf{S}_n^{\mathbf{v}} = \mathbf{0} \tag{178}$$

$$S_e^p = 0 \tag{179}$$

$$S_i^p = \frac{2}{3} N_n N \langle \sigma v \rangle_{ION} \left(\frac{3}{2} k T_n + \frac{1}{2} m_n \mathbf{v}_n^2\right) \tag{180}$$

Compared to the introductory model in Section 11.2.1, spatial variations in background density and cross-section are handled by the null collision method, see Section 11.5.2.

Introducing the (super-)particles newly ionised in time interval Δt, occupying positions $\mathbf{x}_p$ with label p and weight w_p and interaction I:

$$S_e^n V^e \Delta t \approx \Sigma_{pI} w_p \delta_D(\mathbf{x} - \mathbf{x}_p) \tag{181}$$

$$S_i^p V^e \Delta t \approx \frac{2}{3} m_n \Sigma_{pI} w_p \delta_D(\mathbf{x} - \mathbf{x}_p) \frac{1}{2} \mathbf{v}_{n,pI}^2 \tag{182}$$

where the contribution to the energy in a finite element e is a sum over all particle interactions I that have occurred in e. These values are projected on the finite element basis as for charge assignments (δ_D is the Dirac delta function) so that they give rise to source terms

$$S_e^n(\mathbf{x}) V^e \Delta t = \Sigma_{e,p} w_p \phi_{e,\xi}(\mathbf{x}_p) \phi_{e,\xi}(\mathbf{x}) \tag{183}$$

$$S_i^p(\mathbf{x}) V^e \Delta t \approx \frac{1}{3} m_n \Sigma_{e,p} w_p \mathbf{v}_{n,p}^2 \phi_{e,\xi}(\mathbf{x}_p) \phi_{e,\xi}(\mathbf{x}) \tag{184}$$

where $\phi_{e,\xi}$ is the expansion basis as a function of global position $\mathbf{x}$, ie. $\phi_{e,\xi}(\mathbf{x}) = \phi_e(\xi(\mathbf{x}))$, and the mass matrix has been lumped.

11.3 Initial conditions

These are defined separately for the fluid ('continuum') species and the particle species.

11.4 Boundary conditions

Only conditions coupling both particle and fluid species are to specified here, otherwise see separate treatments.

11.4.1 Recycling

Recycling of the plasma reaching the wall implies that the source of neutrals coming from the target plates has a flux (and spatial profile) equal to the flux of ions reaching the target multiplied by some recycling coefficient R_p (eg. a fraction like 0.99). Recycling is a complicated process [10, §9.4] whereby the ions penetrate the solid lattice of the surface, lose significant energy before neutralising and fraction R_p reappears at the surface with a relatively low (below $5\,eV$) temperature.

The flux of ionised plasma from the fluid code is $n\mathbf{v}$, which translates into a total incident number of particles $n|\mathbf{v}|\Delta t \Delta S$, where ΔS is the area of surface impacted, which might be taken as the area of a finite element surface. Thus there are $R_p n|\mathbf{v}|\Delta t \Delta S$ recycled particles to be represented as superparticles. If the superparticles have fixed weight then it might be necessary to use Monte Carlo to treat 'fractional' superparticles, but simple rounding to the nearest integer should meet larger number cases. Otherwise, if there is a reference weight w_{p0} then a set of superparticles should be launched each with a weight close to this value. It will be assumed that these 'recycled' neutrals are born with a Cosine-Knudsen distribution at a user-specified temperature T_{Kn} of a few eV. (Momentum and energy fluxes given by the fluid code may in a simple approximation be disregarded.)

11.5 Calculating particle interactions

11.5.1 Classical scattering

For interactions in which there is significant momentum or energy transfer, it is necessary to do a classical scattering problem to account for the interchange.

For inelastic collisions between two particle of mass m_p and velocity $\mathbf{v}_p$, $p = 1,\ 2$, momentum and energy conservation give

$$
\begin{aligned}
m_1\mathbf{v}_1 + m_2\mathbf{v}_2 &= m_1\mathbf{v}_1^+ + m_2\mathbf{v}_2^+ & (185) \\
m_1\mathbf{v}_1^2 + m_2\mathbf{v}_2^2 &= m_1\mathbf{v}_1^{+2} + m_2\mathbf{v}_2^{+2} & (186)
\end{aligned}
$$

where the velocities $\mathbf{v}_1^+$ and $\mathbf{v}_2^+$ at the new time are found from the observation that momentum conservation is satisfied if $\mathbf{v}_1^+ = \mathbf{v}_1 - \mathbf{p}/m_1, \quad \mathbf{v}_2^+ = \mathbf{v}_2 - \mathbf{p}/m_2$ for any $\mathbf{p}$. Substituting in the energy conservation equation, it follows that $\mathbf{p} = 2\mu_m(\mathbf{v}_1 - \mathbf{v}_2)$ where reduced mass

$$
\mu_m = \frac{m_1 m_2}{m_1 + m_2} \tag{187}
$$

so that

$$
\begin{aligned}
\mathbf{v}_1^+ &= \mathbf{v}_1 - 2\frac{m_2}{m_1 + m_2}(\mathbf{v}_1 - \mathbf{v}_2) & (188) \\
\mathbf{v}_2^+ &= \mathbf{v}_2 + 2\frac{m_1}{m_1 + m_2}(\mathbf{v}_1 - \mathbf{v}_2) & (189)
\end{aligned}
$$

11.5.2 Simplified models

The PIC-MCC software [26] accounts for spatial variations in background density and cross-section by the null collision method, also known as 'delta-tracking'. This method amounts to a correction to the introductory model, relying on the maximum property of the rate $\nu_{\sigma max}$, whereby the number of collisions is reduced according to the local value of $n_e \sigma_{ION}$ in the volume ΔV (which volume might well correspond to that of finite element e). The local value gives a more accurate estimate for p_q. A second random number ξ_2 is drawn from the uniform distribution and the neutral remains unchanged if $\xi_2 < \mathrm{p}_T - \mathrm{p}_q$.

11.5.3 Preferred approach

The "Direct Sampling" approach of Brown and Martin [27] involves the most arithmetic per particle of the techniques considered, but should generally provide increased accuracy which since the arithmetic cost is likely dominated by data movement, comes essentially "free of charge". Note that the sampling techniques needed to treat all 3 interactions mentioned above are common to all, although additional modelling is needed to handle momentum and energy transfer in some interactions. Comparisons of "Direct Sampling" and the algorithm used in PIC-MCC are made in refs [28, 29].
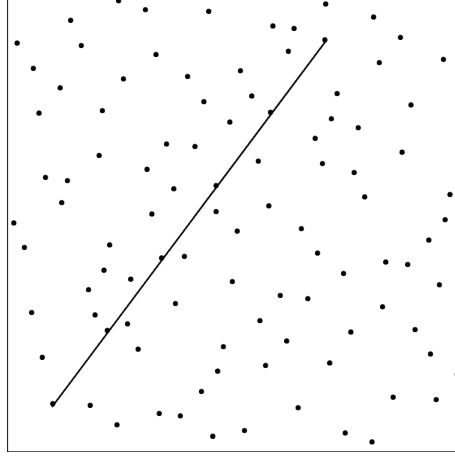
Figure 5: Conceptual configuration. A particle, indicated by the straight line, moves against a background thermal ('fluid') species shown as dots. In the refinement by De Esch, interactions take place at uniformly spaced intervals along the track, also indicated by dots

As illustrated in Figure 5, let $\tau(s)$ be the optical depth traversed by a article traveling a distance s through a medium with arbitrarily specified macroscopic cross-section $\sigma(s)$:

$$\tau(s) = \int_0^s \sigma(s')ds' \tag{190}$$

We assume only that σ is finite and $\sigma(s) \geq 0$. Note that

$$\frac{d\tau}{ds} = \sigma(s) \tag{191}$$

To explicitly allow for the case of no collision in a finite distance of travel, we define P_{NC}, the probability of no collisions, as

$$\mathrm{P}_{NC} = \exp\left(-\tau(\infty)\right) \tag{192}$$

Then the probability density function (pdf) for a collision occurring after a particle has traveled a distance s through the medium is given by [30, §7]

$$\mathrm{p}(s) = \mathrm{P}_{NC}\delta(s - s_\infty) + \frac{d\tau}{ds}\exp\left(-\tau(s)\right) \tag{193}$$

where $\frac{d\tau}{ds}$ is the interaction probability per unit distance travelled, s_∞ is the distance to the boundary of the computational domain and $\exp\left(-\tau(s)\right)$ is the probability of traversing distance s without collision. Equation (193) explicitly allows for cases where $\tau(\infty)$ is finite, hence there is a possibility of traveling an infinite distance without colliding.

Unbiased random sampling of the Monte Carlo path requires solving the following for s, distance along the path, namely

$$\xi = \int_0^s \mathrm{p}(s')ds' \tag{194}$$

where ξ is sampled from a uniform random variable on $[0,1)$. In the spirit of De Esch, values of $\xi = j/N_\xi, j = 1, \ldots N_\xi - 1$ should be used, and the charged particle weights (effectively the

number of physical particles each represents) be reduced by N_ξ. Values of $N_\xi \approx 10 - 100$ are suggested.

In the first step of the sampling, discrete sampling is used to select a collision with probability $(1 - P_{NC})$ or an infinite flight with probability P_{NC}. That is, if $\xi > P_{NC}$, then there is a collision. The second step is to sample s from from the pdf given by:

$$g(s') = \frac{1}{G}\frac{d\tau}{ds'}\exp\left(-\tau(s')\right) \tag{195}$$

where

$$G = (1 - P_{NC}) \tag{196}$$

Using Equation (195), note that

$$\int_0^s g(s')ds' = \frac{1}{G}\int_0^{\tau(s)} \exp\left(-\tau\right)d\tau \tag{197}$$

Using Equations(194) and (195), we can sample $\tau_s = \tau(s)$ by solving

$$\xi = \frac{1}{G}\int_0^{\tau_s} \exp{-\tau}d\tau \tag{198}$$

This is equivalent to sampling from a truncated exponential pdf, which has the solution

$$\tau_s - \ln(1 - G\xi) \tag{199}$$

Pathlength s then follows from Equation (190), viz.

$$\tau_s = \int_0^s \sigma(s')ds' \tag{200}$$

When $\sigma(s')$ has a simple functional form, Equation (200) can often be solved analytically for s. In many cases which arise in practice, the solution may involve a transcendental equation or other form not amenable to analytic solution. Equation (200), however, can be readily solved numerically for s using Newton iteration with $f = \int_0^s \sigma(s')ds' - s$, starting with an initial estimate $s_0 = \tau_s/\sigma(0)$ [27]. Because $df/ds \leq 0$, f is monotone and there can be at most one root. For cases where $\sigma(s') \geq 0$, the Newton iteration is guaranteed to converge. However, if $\sigma(s')$ is zero or very small over a portion of the path, df/ds may be 0, leading to numerical difficulties and nonconvergence. This potential problem is remedied easily by combining Newton with a bisection search method, such that bisection is used if df/ds is very small or zero. Using this approach, Brown and Martin found that only $1 - 5$ iterations are typically needed to converge s to within part in 10^6. even for extreme variations in $\sigma(s')$.

A final practical point concerns the relation of path length s to physical coordinates. If the particle starts at $\mathbf{x}_0$ and travels in a direction given by $\mathbf{v}_p$ parallel to unit vector $\mathbf{d}$ then the particle path is given by

$$\mathbf{x} = \mathbf{x}_0 + s\mathbf{d} \tag{201}$$

so inverting

$$s = |\mathbf{x} - \mathbf{x}_0|/|\mathbf{d}| \tag{202}$$

so it is helpful if $\mathbf{d}$ is a unit vector.

12 Summary

Acknowledgement

References

[1] Proxy Applications. `https://proxyapps.exascaleproject.org`, 2020. Online; accessed May 2020.

[2] W. Arter, L. Anton, D. Samaddar, and R. Akers. ExCALIBUR Fusion Modelling System Science Plan. Technical Report CD/EXCALIBUR-FMS/0001, UKAEA, 11 2019. `https://www.metoffice.gov.uk/binaries/content/assets/metofficegovuk/pdf/research/spf/ukaea-excalibur-fms-scienceplan.pdf`.

[3] E.C. Howell and C.R. Sovinec. Solving the Grad–Shafranov equation with spectral elements. *Computer Physics Communications*, 185(5):1415–1421, 2014. `http://dx.doi.org/10.1016/j.cpc.2014.02.008`.

[4] J.P. Gunn, T. Hirai, Y. Corre, F. Escourbiac, A. Grosjean, and R.A. Pitts. A study of planar toroidal–poloidal beveling of monoblocks on the ITER divertor outer vertical target. *Nuclear Fusion*, 59(12):126043, 2019.

[5] R. Dejarnac, J.P. Gunn, P. Vondracek, M. Komm, R. Panek, and R.A. Pitts. Physics of toroidal gap heat loading on castellated plasma-facing components. *Nuclear Materials and Energy*, 19:19–27, 2019.

[6] Code generation QPROG style, example of Braginskii plasma transport coefficients. `https://github.com/wayne-arter/smardda-misc`, 2017. Accessed: December 2020.

[7] J.D. Huba. NRL Plasma Formulary. Technical Report NRL/PU/6790–07-500, Naval Research Laboratory, Washington, 2007. Online version dated 2009 at `https://apps.dtic.mil/dtic/tr/fulltext/u2/a499299.pdf`.

[8] S.I. Braginskii. Transport Processes in a Plasma. In M.A.Leontovich, editor, *Reviews of Plasma Physics Vol.1*, pages 205–311. Consultants Bureau, New York, 1965.

[9] J.P. Goedbloed and S. Poedts. *Principles of magnetohydrodynamics: with applications to laboratory and astrophysical plasmas*. Cambridge University Press, 2004.

[10] J.A. Wesson. *Tokamaks, 3rd Edition*. Clarendon Press, Oxford, 2003.

[11] P.H. Roberts. *An Introduction to Magnetohydrodynamics*. Longmans, London, 1967.

[12] L.C. Appel, I. Lupelli, and JET Contributors. Equilibrium reconstruction in an iron core toka-mak using a deterministic magnetisation model. *Computer Physics Communications*, 223:1–17, 2018.

[13] E. Havlíčková, W. Fundamenski, F. Subba, D. Coster, M. Wischmeier, and G. Fishpool. Benchmarking of a 1D scrape-off layer code SOLF1D with SOLPS and its use in modelling long-legged divertors. *Plasma Physics and Controlled Fusion*, 55(6):065004, 2013.

[14] W.T. Taitano, D.A. Knoll, L. Chacón, and G. Chen. Development of a Consistent and Stable Fully Implicit Moment Method for Vlasov–Ampère Particle in Cell (PIC) System. *SIAM Journal on Scientific Computing*, 35(5):S126–S149, 2013.

[15] G. Chen, L. Chacón, and D.C. Barnes. An energy-and charge-conserving, implicit, electro-static particle-in-cell algorithm. *Journal of Computational Physics*, 230(18):7018–7036, 2011.

[16] V.M. Zhdanov. *Transport processes in multicomponent plasma*. CRC Press, 2002.

[17] W.B. Thompson. *An Introduction to Plasma Physics*. Pergamon, 1962.

[18] Hermes plasma edge simulation model: Hermes-3, a hot ion multifluid drift-reduced model. `https://github.com/bendudson/hermes-3`, 2021. Accessed: June 2021.

[19] P.C. Stangeby. *The plasma boundary of magnetic fusion devices*. Taylor & Francis, New York, 2000.

[20] J.J. Duderstadt and W.R. Martin. *Transport Theory*. Wiley, 1979.

[21] R.W. Hockney and J.W. Eastwood. *Computer Simulation Using Particles*. IOP Publishing, 1988.

[22] H. Niederreiter. *Random Number Generation and Quasi-Monte Carlo Methods*. Society for Industrial Mathematics, 1992.

[23] M.H. Kalos and P.A. Whitlock. *Monte Carlo Methods. Vol. 1: basics*. Wiley-Interscience New York, NY, USA, 1986.

[24] F. I. Parra, M. Barnes, and M. Hardman. 2D drift kinetic models with wall boundary conditions. Technical Report 2047357-TN-07-01, UKAEA Project Neptune, 2021. `https://github.com/ExCALIBUR-NEPTUNE/Documents/blob/main/reports/2047357/TN-07.pdf`.

[25] The ADAS Project. Atomic Data and Analysis Structure ADAS website. `http://www.adas.ac.uk/`, 2020. Accessed: July 2020.

[26] J.P. Verboncoeur. Particle simulation of plasmas: review and advances. *Plasma Physics and Controlled Fusion*, 47(5A):A231–A260, 2005.

[27] F.B. Brown and W.R. Martin. Direct Sampling of Monte Carlo Flight Paths in Media with Con-tinuously Varying Cross-sections. In *ANS Mathematics and Computation Topical Meeting, Gatlinburg, TN, April*, pages 6–11, 2003.

[28] Z. Li, K. Wang, and X. Zhang. Research on applying neutron transport Monte Carlo method in materials with continuously varying cross sections. 2011. `https://inis.iaea.org/collection/NCLCollectionStore/_Public/48/022/48022323.pdf`.

[29] H. Belanger, D. Mancusi, and A. Zoia. Review of Monte Carlo methods for particle transport in continuously-varying media. *The European Physical Journal Plus*, 135(11):1–22, 2020.

[30] E.E. Lewis and W.F. Miller Jr. *Computational Methods of Neutron Transport*. American Nuclear Society, La Grange Park, Il, 1993.

[31] L. Golub and J.M. Pasachoff. *The solar corona, 2nd Edition*. Cambridge University Press, 2010.

[32] V.A. Ambartsumyan, editor. *Theoretical Astrophysics, translated by J.B.Sykes*. Pergamon Press, 1958.

[33] M. O'Mullane. Atomic Processes in Plasmas. Slides from 45th Culham Plasma Physics Summer School, 2008. CCFE intranet, not publicly available.

[34] R.J. Bray and R.E. Loughhead. *Sunspots*. Dover Publications, 1964.

[35] The ADAS Project. Dissemination of atomic data and analysis structure adas website. `https://open.adas.ac.uk/`, 2020. Accessed: July 2020.

[36] Gwyn Williams. Electron Binding Energies. `https://userweb.jlab.org/~gwyn/ebindene.html`, 2000. Accessed: July 2020.

[37] H. Summers, M. O'Mullane, and A. Whiteford. ADAS: Atomic data, modelling and analysis for fusion. `https://icamdata2006.obspm.fr/documents/icam_pdf/Summers.pdf`, 2006. Slides from Meudon.

[38] N.R. Badnell, M.G. O'Mullane, H.P. Summers, Z. Altun, M.A. Bautista, J. Colgan, T.W. Gorczyca, D.M. Mitnik, M.S. Pindzola, and O. Zatsarinny. Dielectronic recombination data for dynamic finite-density plasmas-I. Goals and methodology. *Astronomy & Astrophysics*, 406(3):1151–1165, 2003.

[39] J.-Ch. Sublet, J.W. Eastwood, J.G. Morgan, M.R. Gilbert, M. Fleming, and W. Arter. FISPACT-II: An Advanced Simulation System for Activation, Transmutation and Material Modelling. *Nuclear Data Sheets*, 139:77–137, 2017. `http://dx.doi.org/10.1016/j.nds.2017.01.002`, website: `https://fispact.ukaea.uk/`.

[40] S.S. Henderson, M. Bluteau, A. Foster, A. Giunta, M.G. O'Mullane, T. Pütterich, and H.P. Summers. Optimisation and assessment of theoretical impurity line power coefficients relevant to ITER and DEMO. *Plasma Physics and Controlled Fusion*, 59(5):055010, 2017.

[41] S.S. Henderson, M.M. Bluteau, M.G. O'Mullane, and H.P. Summers. Improvements of impurity line ITER and DEMO via systematic optimisation of atomic structure. Technical Report UKAEA-CCFE-PR(18)31, CCFE, 2018.

[42] W. Arter. Equations for EXCALIBUR/NEPTUNE Proxyapps. Technical Report CD/EXCALIBUR-FMS/0021-1.00-M1.2.1, UKAEA, 03 2020. `https://github.com/ExCALIBUR-NEPTUNE/Documents/blob/main/reports/ukaea_reports/CD-EXCALIBUR-FMS0021-1.00-M1.2.1.pdf`.

[43] G. Karniadakis and S. Sherwin. *Spectral/hp element methods for computational fluid dynamics 2nd Ed.* Oxford University Press, 2005. `https://doi.org/10.1093/acprof:oso/9780198528692.001.0001`.

[44] W. Arter, E. Threlfall, and J. Parker. Report on user layer design for Uncertainty Quantification. Technical Report CD/EXCALIBUR-FMS/0024-M3.1.3, UKAEA, 10 2020. `https://github.com/ExCALIBUR-NEPTUNE/Documents/blob/main/reports/ukaea_reports/CD-EXCALIBUR-FMS0024-M3.1.3.pdf`.

A   Annex A: Atomic and Molecular Effects

Often the radiation emitted and absorbed by atoms in different ionisation states must be accounted for. There is a compact introduction in Golub and Pasachoff [31, §3.3.1]. This explains how in principle, given a "particular mixture of elements at a specified temperature . . . the number of atoms per unit volume of the gas which are in a particular ionisation state may be calculated . . . then for that atom which emission lines are emitted" and so on for all other constituents of the mixture. (Temperature refers to a black-body radiation field in which the atoms are assumed to sit.) "The sum total of all these bound-bound emissions, plus the bound-free and free-free emissions" is the spectrum, where it is explained that 'bound' and 'free' describe the state of the electron involved in the formation of the line with respect to the atom. But "in practice, carrying out this calculation is . . . enormously complicated".

The complication follows from the range of competing mechanisms even within atoms of one element, namely the bound-bound mechanisms of decay and excitation described in ref [31, §3.2.1], and bound-free of recombination and photo-emission, because of the different possible degrees of ionisation as atomic number A increases and because the proportion of atoms in each ionisation state depends on the proportions in the others.

Ambartsumyan [32, §5] explains at greater length the calculation in *thermal equilibrium* of the proportion of different ions for each element [32, §5.2], then the bound-free / free-bound coefficients (§5.3—§5.5) and free-free (§5.6). In [32, §24.1–24.2] there is a discussion of metastable states, which in the astrophysical context are crucial for the formation of forbidden lines in nebulae, but may also be important in the context of fusion because these metastable atomic states can survive for many seconds at low densities of matter and of radiation. By metastable state is meant that no transition to it from lower energy levels of the electrons is possible except for the so-called 'forbidden', less probable electric quadrupole interactions from the quantum-mechanical matrix elements.

The above outlines the main physics issues. From O'Mullane's slides at the 2008 Summer School [33], the main difference between astrophysics and fusion application seems to be that in the plasma context, if it is used, Saha's ionisation formula needs modification by the Saha-Boltzmann deviation factors b_n or 'b-factors' ref [33, slide 21]. The Zeeman effect is also neglected,

although this might be expected to be important, as from its use in sunspot observation [34, §5.2] spectral line splitting by wavelengths of $0.1\,\text{nm}$ is expected.

The key observation is from O'Mullane [33] that in tokamak modelling, there are two distinct uses for atomic data - (1) to calculate source (loss) terms for species time evolution equations, and (2) to compute synthetic spectra, ie. intensity as a function of frequency. The latter (2) is by far the more involved but it is only critical for diagnosticians working with particular apparatus. Indeed, Golub and Pasachoff [31, §3.3.2] go on to argue that for an optically thin plasma, the radiation (in W/m^3) could be expressible as simply as

$$\mathcal{E}_R = n_e n_p P(T) \tag{203}$$

where n_p accounts for the number density of the plasma ions and $P(T)$ is the emitted power integrated over all wavelengths for a plasma with a specified mix of elements. The separate functions used to compute $P(T)$ depend mainly on electron temperature with a weak dependence on density. The form of $P(T)$ as a result of the integration over spectrum always seems to be smooth. It would seem to be a prime candidate for precomputation as a function of the fractions of the major plasma species, and could be approximated very efficiently because of the smoothness.

O'Mullane [33] give a more detailed result, namely that there is a source/sink term for electron energy of form

$$S^{\mathcal{E}} = -\mathcal{E}_R = n_e \left(\sum_s \sum_{Z=0}^{Z=Z_0(s)} P^Z n^Z - I^Z \left(\mathcal{S}^{Z \to Z_p} n^Z + \alpha^{Z_p \to Z} n^{Z_p} \right) \right) \tag{204}$$

where Z is charge state, the suffix s on the density has been dropped, $Z_m = Z - 1$, $Z_p = Z + 1$, and where $Z_0(s)$ is the number of charge states of species s included in the model. It may be inferred that

$$\mathcal{S}^{Z_m \to Z} \text{ or } \mathcal{S}^{Z \to Z_p} = \text{ ionisation coefficient} \tag{205}$$

$$\alpha^{Z \to Z_m} \text{ or } \alpha^{Z_p \to Z} = \text{ partial dielectronic recombination rate coefficient} \tag{206}$$

$$P^Z = \text{ radiated power per atom of } n^Z \tag{207}$$

$$I^Z = \text{ power per atom released in dielectronic recombination} \tag{208}$$

where the coefficients, as elsewhere in this section, are expected to be obtained from the Atomic Data and Analysis Structure ADAS database [25, 35]. The data requirements for this look relatively modest, assuming the coefficients for each species and charge state are smooth functions of temperature only. Thus if say $N_T \approx 20$ samples specify these functions and $Z_{sum} = \sum_s Z_0(s)$, then the total number of coefficients required could be estimated as $Z_{sum} \times 3 \times N_T \approx 20 \times 3 \times 10 = 600$ where if the number of different elements present $N_s = 10$, and if the average number of charge states $\bar{N}_Z = 2$, then $Z_{sum} = N_s \bar{N}_Z \approx 20$. In another case of interest, a calculation might include only two or three extra species if one were Tungsten (W), so $N_s = 4$ but then $N_Z = 22$ for W alone if $T_e > 40\,\text{eV}$ [36].

The number densities n^Z for each charge state may be straightforwardly calculated by solving a transport equation for each isotope n_s and using the Saha-Boltzmann formula modified with b-factors to determine the distribution of charge states. (Further, for heavier elements a mean atomic mass may be used to avoid separate treatment of isotopic species.) Much more serious

implications for computation [33], arise in the time evolution equations if each charge state is treated separately. This may be necessary in a strong electric field because each different ion feels a different electromagnetic force. An ion of species s with charge state Z will acquire a source

$$S_s^Z = \mathcal{S}^{Z_m \to Z} n_e n^{Z_m} - \left(\alpha^{Z \to Z_m} + \mathcal{S}^{Z \to Z_p} \right) n_e n^Z + \alpha^{Z_p \to Z} n_e n^{Z_p} \tag{209}$$

where again the suffix s on the density has been dropped. Thus the demands on atomic data are not very different from those for the energy equation, but since the total cost of these additional computations with $Z_0(s)$ extra species will scale at least as fast as $Z_{sum} = \sum_s Z_0(s)$ (inter-species coupling may add considerably to the computational expense), rendering negligible the cost of inputting a few thousand coefficients from disc. In practice a useful surrogate is produced by replacing separate ionisation states by 'superstages' (slide 17 of ref [37]), where one superstage corresponds to one electron shell of the atom. However, even the smaller number of 7 superstages required for W might double or treble the length of a typical computation.

The above is typically as much detail as is sensible to consider under heading (1). If detailed diagnostics under (2) are required, the generalised collisional-radiative (GCR) model [38] gives an idea of the computational demands. GCR modelling requires each metastable state to be considered separately, since each has a separate finite lifetime. It helps that the transport of each atom in the state is presumably the same, but even so there is a need to solve a rate equation for metastable state density at sample points throughout the computational domain The source terms are complicated, namely for the metastable state labelled ρ

$$S_\rho^Z / n_e = \sum_\sigma \mathcal{X}_{\sigma \to \rho}^{Z \to Z} n_\sigma - \sum_\sigma \mathcal{X}_{\rho \to \sigma}^{Z \to Z} n_\rho \tag{210}$$

$$+ \sum_\mu \mathcal{S}_{\mu \to \rho}^{Z_m \to Z} n_\mu^{Z_m} - \sum_\nu \mathcal{S}_{\rho \to \nu}^{Z \to Z_p} n_\rho \tag{211}$$

$$+ \sum_\nu \alpha_{\nu \to \rho}^{Z_p \to Z} n_\nu^{Z_p} - \sum_\mu \alpha_{\rho \to \mu}^{Z \to Z_m} n_\rho \tag{212}$$

$$+ \sum_\sigma \mathcal{Q}_{\sigma \to \rho}^{Z \to Z} n_\sigma - \sum_\sigma \mathcal{Q}_{\rho \to \sigma}^{Z \to Z} n_\rho \tag{213}$$

where the superfix Z as well as the suffix s on the density has been dropped and the new symbols are

$$\mathcal{X}_{\sigma \to \rho}^{Z \to Z} = \text{generalised collisional-radiative (GCR) excitation coefficient} \tag{214}$$

$$\mathcal{Q}_{\sigma \to \rho}^{Z \to Z} = \text{parent-metastable cross-coupling coefficient} \tag{215}$$

Note that the expressions in both ref [38, eq. (9)] and ref [33, slide 41] appear to contain typos, and that the meanings of $\mathcal{X}$ and $\mathcal{Q}$ have swapped. Each of the new terms contains approximately $8M_Z$ coefficients where M_Z is the number of metastable states for species s (which includes the ground state). It may be inferred from refs [33, 37] that the number of metastable states for a given ionisation Z is relatively small (slide 9 of ref [37] indicates that all ionisation states for Oxygen have $M_Z \leq 4$; slide 19 suggests $M_Z \leq 6$ for W when $T_e < 100$ eV). The coefficients $\mathcal{X}, \mathcal{S}, \mathcal{Q}$ in Equation (210) are functions of electron density as well as temperature so may require at least 100 sample points to specify, hence the total data can be estimated as $Z_{sum} \times M_Z \times 8M_Z \times 100$. However FISPACT-II [39] experience with rate equations indicates the cost of these additional computations

with M_Z metastables far exceeds the cost of inputting of order ten or so thousand coefficients from disc.

Where the demands of data might become important is in the translation of the n_σ^Z into spectral lines. First the regular excited states, because they equilibrate on the usual atomic timescales which are negligible compared to plasma timescales, are calculated using a purely algebraic relation [38, eq. (5)],

$$n_i^Z/n_e = \sum_\sigma {}^X\mathcal{F}_{i\sigma}n_\sigma^Z + \sum_\mu {}^I\mathcal{F}_{i\mu}n_\mu^{Z_m} + \sum_\nu {}^R\mathcal{F}_{i\nu}n_\nu^{Z_p} \tag{216}$$

where ${}^{X,I,R}\mathcal{F}_{i\sigma}$ are the coefficients of excitation, ionisation and recombination for the transition from metastable state σ to regular excited state i, each is a function of n_e and T_e with corresponding storage requirement of order 100. Equation (216) requires $Z_{sum} \times M_S \times M_Z$ $\mathcal{F}$ coefficients where M_S is the number of states, which is potentially infinite, and indeed in practice could be as large as ≈ 500, necessitating the use of 'bundling' of the higher energy states to reduce the number to manageable proportions, say 10 [38]. Next, as explained in the opening paragraph, to each state there corresponds a description of its spectrum, which may contain many separate lines, each described by its wavelength, relative amplitude and a profile shape which may require several further parameters to describe. Mitigating the demand for coefficient data, is the fact that the diagnostics need only be computed intermittently.

To treat atomic physics UQ in a later stage of NEPTUNE, a Monte-Carlo calculation might be considered, involving all the different interactions between all the metastable states where the Maxwellian assumption is relaxed, posing a multiscale multiphysics problem. However, the validity of this approach requires further consideration as Henderson et al [40] also indicates that even as recently as 2017, errors of 30 % were present in important coefficients, although the discrepancies have now been reduced to approximately 5 % [41].

B   Annex B: Index of Mathematics

Table 1: **TABLE OF MATHEMATICAL SYMBOLS** If no units are given, then quantity is dimensionless, or if the units are given as ?, then the dimensions depend on context. Generally, the usage of symbols tries to follow that from the Plasma Formulary [7], in SI units, with temperatures specified as kT which returns J. The Formulary also give the fundamental dimensions of the SI units, which should enable checking of dimensional consistency of equations, eg. magnetic field induction is in Tesla (T) whence the fundamental dimension expression gives $T = kgs^{-1}C^{-1}$. Note that the symbols are sorted by font as well as alphabet, so that boldface symbols appear immediately after 'b' (backslashes ignored). The main source for the symbols is the Equations document [42], also included are those listed as used in the text by Karniadakis and Sherwin [43], prefaced by (K+S), plus symbols used in the report [44].

Symbol	Description	Units
a	minor radius of the torus (horizontal)	m
a_{ij}	coefficient of matrix A	
A	atomic mass of the ion	
$[a, b]$	arbitrary finite interval	
α	as suffix is species label or index	
α_n	perturbation amplitude	
$\alpha^{Z_p \to Z}$	partial dielectronic recombination rate coefficient	$m^3 s^{-1}$
$\alpha^{Z \to Z_m}$	partial dielectronic recombination rate coefficient	$m^3 s^{-1}$
b	minor radius of the torus (vertical)	m
B_0	used to make B dimensionless	T
B_s	characteristic magnetic field used to make $\mathbf{B}$ dimensionless	T
$\bar{N}_Z$	average number of charge states	
$B = |\mathbf{B}|$	amplitude of the imposed magnetic field	T
B_T	amplitude of the imposed toroidal magnetic field	T
β	as suffix is species label	
β	(Glossary) Ratio of plasma pressure to pressure in magnetic field	
$\mathbf{a} = d^2\mathbf{x}/dt^2$	acceleration experienced by a particle	$m^2 s^{-1}$
$\mathbf{A}(\mathbf{x}, t)$	magnetic vector potential	Tm
$\mathbf{B}(\mathbf{x}, t)$	magnetic field	T
$\mathbf{b}$	unit vector giving the direction of the magnetic field	
$\mathbf{E}(\mathbf{x}, t)$	electric field	Vm^{-1}
E_s	characteristic electric field used to make $\mathbf{E}$ dimensionless	Vm^{-1}
$\mathbf{E}^+$	modified electric field	m^{-2}
$\mathbf{F}$	force vector	N
$\mathbf{u}_\wedge$	pseudo / thermal velocity component in flux surface normal to field direction	ms^{-1}
$\mathbf{v}$	generic velocity	ms^{-1}

$\mathbf{v}_\alpha$		velocity of species α	ms^{-1}
$\mathbf{v}_\parallel$		fluid velocity component along fieldline	ms^{-1}
$\mathbf{v}_\perp$		fluid velocity component normal to flux surface	ms^{-1}
$\mathbf{v}_\wedge$		fluid velocity component in flux surface normal to field direction	ms^{-1}
$\mathbf{v}_0$		initial fluid velocity	ms^{-1}
$\mathbf{v}_{cx}$		'charge exchange' perpendicular fluid velocity component	ms^{-1}
$\mathbf{v}_{E\times B}$		'E cross B' perpendicular fluid velocity component	ms^{-1}
$\mathbf{v}_e$		velocity of the electrons	ms^{-1}
$\mathbf{v}_i$		velocity of the ion species	ms^{-1}
$\mathbf{v}_{\nabla Be}$		'grad B' perpendicular fluid velocity component for electrons	ms^{-1}
$\mathbf{v}_{\nabla Bi}$		'grad B' perpendicular fluid velocity component for ions	ms^{-1}
$\mathbf{v}_{\mathrm{diff}}$		'diffusive' perpendicular fluid velocity component	ms^{-1}
$\mathbf{x}$ $(x_1, x_2, \ldots, x_d)$	$=$	is a d-dimensional vector	
$\mathbf{x}$		position	m
b_n		'b-factors' ref [33, slide 21]	
$\xi(\theta)$		multi-dimensional random variable with a specific probability distribution as a function of the random parameter $0 \leq \theta \leq 1$	
$\boldsymbol{B}$		(K+S) Basis matrix	
$\boldsymbol{D}_\xi$		(K+S) Elemental derivative matrix with respect to ξ	
$\boldsymbol{f}^e$		(K+S) Force vector of the eth element	
$\boldsymbol{H}$		(K+S) Helmholtz matrix $(= \mathcal{A}^T \underline{\boldsymbol{H}}^e \mathcal{A}))$	
$\boldsymbol{H}^e$		(K+S) Elemental Helmholtz matrix	
$\boldsymbol{L}$		(K+S) Laplacian matrix $(= \mathcal{A}^T \underline{\boldsymbol{L}}^e \mathcal{A}))$	
$\boldsymbol{\Lambda}(u)$		(K+S) Diagonal matrix of $u(\xi_i, \xi_2)$ evaluated at quadrature points	
$\boldsymbol{L}^e$		(K+S) Elemental Laplacian matrix	
$\boldsymbol{M}$		(K+S) Mass matrix $(= \mathcal{A}^T \underline{\boldsymbol{M}}^e \mathcal{A})$	
$\boldsymbol{\mathcal{A}}^T$		(K+S) Matrix global assembly	
$\boldsymbol{M}^e$		(K+S) Elemental mass matrix	
$\boldsymbol{n}$		(K+S) Unit outward normal	
$\boldsymbol{\omega}$		(K+S and plasma models) Vorticity	s^{-1} or Cm^{-3}
$\boldsymbol{u}^e$		(K+S) Vector containing function evaluated at quadrature points	
$\boldsymbol{W}$		(K+S) Diagonal weight / Jacobian matrix	
$\xi(\theta)$		multi-dimensional random variable with a specific probability distribution as a function of the random parameter $0 \leq \theta \leq 1$	
B_p		amplitude of the poloidal magnetic field	T
$C_0 = \sqrt{K_{MA} T_0}$		used to make velocities dimensionless	ms^{-1}
$\cap$		(Sets) Set intersection	
χ		(K+S) Space of trial solutions	
χ^δ		(K+S) Finite-dimensional space of trial solutions	
$\chi_i(\xi)$		(FE Basis) Local Cartesian to global coordinate mapping	

c_p	specific heat at constant pressure	$Jkg^{-1}K^{-1}$
$c_s = \sqrt{\frac{kT_i + Z_i kT_e}{m_i}}$	approx. plasma acoustic speed	ms^{-1}
$c_s = \sqrt{\frac{p}{\rho_m}}$	plasma acoustic speed	ms^{-1}
$c_{se} = \sqrt{\frac{kT_e}{m_e}}$	acoustic speed of electrons	ms^{-1}
$c_{si} = \sqrt{\frac{kT_i}{m_i}}$	acoustic speed of ions	ms^{-1}
C_S	sound speed coefficient in radiation equation	ms^{-1}
$\cup$	(Sets) Set union	
$C(x_i, x_j)$	covariance of random variables x_i, x_j	
d	number of dimensions over which the integral is performed	
δp_i	stress tensor	Nm^{-2}
δ	Kronecker delta	
δ_D	Dirac delta function	
δ_e	energy flux factor at boundary of the electrons	
$\delta = \frac{1}{2}(\delta_e + \delta_i)$	energy flux factor at boundary of 'mean' species	
δ_i	energy flux factor at boundary of the ion species	
δ_α	(Glossary) Magnetisation parameter, species α gyroradius normalised to L	
$\delta(x)$	Dirac delta function of continuous real variable x	
D	spatial dimensionality of problem	
D_A	diffusion coefficient for plasma charges in a background of neutrals	$m^2 s^{-1}$
D_e	diffusion coefficient for electrons in a background of neutrals	$m^2 s^{-1}$
$D_{fv\alpha}$	scale dissipation in equation for evolution of species velocity $\mathbf{v}_\alpha$	
D_n	neutral diffusion coefficient	$m^2 s^{-1}$
$D_{fp\alpha}$	scale dissipation in equation for evolution of species pressure/energy p_α	
D_i	diffusion coefficient for ions in a background of neutrals	$m^2 s^{-1}$
$|e|$	absolute value of the charge on the electron	C
e	(K+S) Finite element number $1 \leq e \leq N_{el}$	
e_{ijk}	weighted integral of triple products of Ψ_i of the ion species	
$\emptyset$	(Sets) Empty set	
ϵ_0	permittivity of free space	Fm^{-1}
$\epsilon_r = t_s/t_0$	scale factor for transient term	
η_1, η_2, η_3	(FE Basis) Local collapsed Cartesian coordinates	
η_B	plasma resistivity after Braginskii	Ωm
$\eta_d = \eta_B/\mu_0$	plasma resistivity, as diffusivity	$m^2 s^{-1}$
η_{en}	contribution to plasma resistivity, as diffusivity, from electron-neutral interactions	$m^2 s^{-1}$
$\eta_{en\parallel}$	contribution to plasma parallel resistivity, as diffusivity, from electron-neutral interactions	$m^2 s^{-1}$
η_{in}	contribution to plasma resistivity, as diffusivity, from ion-neutral interactions	$m^2 s^{-1}$

$\eta_{in\parallel}$	contribution to plasma parallel resistivity, as diffusivity, from ion-neutral interactions	$m^2 s^{-1}$
f_0	constant in the expansion of $f(x_1, \ldots, x_d)$	
f_0	initial distribution function of the electrons	$m^{-6} s^3$
f_α	distribution function of species α	$m^{-6} s^3$
f_e	distribution function of the electrons	$m^{-6} s^3$
f_i	distribution function of the ion species	$m^{-6} s^3$
$f_{ij}(x_i, x_j)$	coefficient in the expansion of $f(x_1, \ldots, x_d)$	
$f_{ce} = \frac{\omega_{ce}}{2\pi}$	electron cyclotron frequency	s^{-1}
$f_{ci} = \frac{\omega_{ci}}{2\pi}$	ion cyclotron frequency	s^{-1}
$f_{pe} = \frac{\omega_{pe}}{2\pi}$	electron plasma frequency	s^{-1}
$f_{pi} = \frac{\omega_{pi}}{2\pi}$	ion plasma frequency	s^{-1}
$f_i(x_i)$	coefficient in the expansion of $f(x_1, \ldots, x_d)$	
$f(x_1, \ldots, x_d)$	joint probability distribution	
$f^{\mathcal{E}}$	flux term (fieldline integrated source) for plasma energy	
$F^{\mathcal{E}}$	flux term (fieldline integrated source divided by field) for plasma energy	$m^{-1} s^{-2} C$
f^n	flux term (fieldline integrated source) for plasma number density	
F^n	flux term (fieldline integrated source divided by field) for plasma number density	$m^{-3} C$
f^u	flux term (fieldline integrated source) for plasma momentum	
F^u	flux term (fieldline integrated source divided by field) for plasma momentum	$m^{-2} s^{-1} C$
$f(x, \mathbf{v}, t)$	generic distribution function	$m^{-6} s^3$
$f_{n,Kn}(\mathbf{v})$	Knudsen distribution function	$m^{-4} s^4$
$\Gamma(x)$	gamma function of continuous variable x	
$g(h_j)$	activation function (of input h_j) of a neuron in a neural network	
G	Green's function	
H_α	Hamiltonian for species α	
$\hat{\boldsymbol{u}}^e$	(K+S) Vector of expansion coefficients	
$\hat{v}_g$	(K+S) Global list of coefficients	
$\hat{v}_g$	(K+S) List of all elemental coefficients ($= \underline{v}^e$)	
h_j	real-number input to a neuron in a neural network	
$h_p(\xi)$	(FE Basis) One-dimensional Lagrange polynomial of order p	
i	as suffix denotes ions	
i	as suffix denotes regular excited state	
i	as suffix generic label	
I	as suffix labels Monte-Carlo interactions	
I_ϕ	$\phi-$ or toroidal component of plasma current	A
I_H	Hydrogen reionisation potential as defined in ref [13]	eV
i, j, k	(K+S) General summation indices	
$^I\mathcal{F}_{i\sigma}$	coefficient of ionisation for the transition from metastable state σ to regular excited state i	

$\in$	(Sets) Is a member of; belongs to	
$I(\psi) = B_T/R$	function giving the toroidal field as a function of ψ	Tm^{-1}
I^Z	power per atom released in dielectronic recombination	W
j	as suffix is generic label	
$j_{ext}(R, Z)$	electric current density induced in plasma by external coils	Am^{-2}
j_ϕ	$\phi-$ or toroidal component of plasma current density	Am^{-2}
$\mathbf{j}_{sh}$	sheath plasma current density	Am^{-2}
k	as suffix is generic label	
k	chosen to scale so that kT_0, kT_d is an energy	?
κ_α	thermal diffusivity of species α	m^2s^{-1}
$\kappa_{e\parallel}$	parallel thermal diffusivity of electrons	m^2s^{-1}
$\kappa_{e\perp}$	perpendicular thermal diffusivity of electrons	m^2s^{-1}
$\kappa_{i\parallel}$	parallel thermal diffusivity of ions	m^2s^{-1}
$\kappa_{i\perp}$	perpendicular thermal diffusivity of ions	m^2s^{-1}
$\kappa = k_c/\rho_m c_p$	thermal diffusivity tensor of solid	m^2s^{-1}
k_B	Boltzmann's constant	JK^{-1}
k_c	thermal conductivity tensor	$Jm^{-1}s^{-1}K^{-1}$
$K_{cx}(n_i, T_i)$	reaction rate of charge exchange reactions	m^3s^{-1}
K_i	ionization reaction rate	m^3s^{-1}
K_{MA}	chosen as k_B/m_i or $|e|/m_i$ so that $\sqrt{K_M T_d}$ is an ion speed	?
K_M	chosen as k_B/m_u or $|e|/m_u$ so that $\sqrt{K_M T_d/A}$ is an ion speed	?
K_r	recombination reaction rate	m^3s^{-1}
kT_0	T_0 in energy units	J
kT_d	T_d in energy units	J
$K_v(x)$	modified Bessel function of the second kind, order v	
k_w	wavenumber vector	m^{-1}
λ	arbitrary quantity	?
λ	Coulomb logarithm	
λ	(K+S) Helmholtz equation constant	
Λ	Coulomb logarithm	
λ_q	e-folding length of midplane profile of power loss when an exponential is fitted	m
Λ_b	sheath potential drop normalized to T_e	eV
λ_D	(Glossary) Debye lengthscale above which local electrostatic fluctuations due to presence of discrete charged particles are negligible	m
$\lambda_{\alpha mfp}$	(Glossary) Mean free path of particle species α	m
$\langle \sigma v \rangle_{CX}$	reaction rate for charge exchange	m^3s^{-1}
$\langle \sigma v \rangle_{ION}$	reaction rate for ionisation	m^3s^{-1}
$\langle \sigma v \rangle_{REC}$	reaction rate for recombination	m^3s^{-1}
$\langle \sigma v \rangle$	generic reaction rate	m^3s^{-1}
L_0	Typical lengthscale	m
$L_i^{N_m}(\boldsymbol{\xi})$	(FE Basis) Two-dimensional Lagrange polynomial through N_m nodes ξ_i	
L_s	Typical lengthscale along fieldline	m

Symbol	Description	Units
m	species particle mass	kg
M_0	Mach number at $s = 0$ boundary	
M_1	Mach number at $s = 1$ boundary	
m_α	mass of species α	kg
$\mathbb{E}$	expectation	
$\mathbb{E}_{k \neq i, l \neq j}$	expectation computed by integrating over all the x_k except for x_i and x_j	
$\mathbb{E}_{x_{k \neq i}}$	expectation computed by integrating over all the x_k except for x_i	
$\mathbb{L}(u)$	(K+S) Linear operator in u	
$\mathbb{P}$	(K+S) Projection operator	
$\mathbb{P}^\delta$	(K+S) Discrete projection operator	
$\mathbf{v}$	(K+S) Velocity $[u, v, w]^T$	
$\mathcal{E}_\alpha$	energy of species α	Jm^{-3}
$\mathcal{E}_e$	energy of the electrons	Jm^{-3}
$\mathcal{E}_i$	energy of the ion species	Jm^{-3}
$\mathcal{E}_R$	total plasma radiation	Wm^{-3}
$\mathcal{F}$	generic coefficient of excitation, ionisation or recombination	$m^3 s^{-1}$
$\mathcal{F}_\alpha$	functional of moments of species α	$m^{-6} s^3$
$\mathcal{I}$	(K+S) Interpolation operator	
$\mathcal{I}^\delta$	(K+S) Discrete interpolation operator	
$\mathcal{K}_\parallel$	parallel thermal conductivity of plasma	$m^{-1} s^{-1}$
$\mathcal{K}$	thermal conductivity of plasma	$m^{-1} s^{-1}$
$\mathcal{K}_\perp$	thermal conductivity of plasma perpendicular to field and flux surface	$m^{-1} s^{-1}$
$\mathcal{K}_\wedge$	thermal conductivity of plasma perpendicular to field in flux surface	$m^{-1} s^{-1}$
$\mathcal{L}_7$	7-D Lie derivative (space, velocity-space and time make up the $3 + 3 + 1 = 7$ dimensions)	s^{-1}
$\mathcal{P}_P(\Omega)$	(K+S) Polynomial space of order P over Ω	
$\mathcal{Q}$	coefficient in radiation equation	$m^3 s^{-1}$
$\mathcal{Q}_{\sigma \to \rho}^{Z \to Z}$	parent-metastable cross-coupling coefficient	$m^3 s^{-1}$
$\mathcal{S}$	coefficient in radiation equation	$m^3 s^{-1}$
$\mathcal{S}^{Z_m \to Z}$	ionisation coefficient	$m^3 s^{-1}$
$\mathcal{S}^{Z \to Z_p}$	ionisation coefficient	$m^3 s^{-1}$
$\mathcal{T}$	generic tensor	?
$\mathcal{V}$	(K+S) Space of test functions	
$\mathcal{V}^\delta$	(K+S) Finite-dimensional space of test functions	
$\mathcal{X}$	coefficient in radiation equation	$m^3 s^{-1}$
$\mathcal{X}_{\sigma \to \rho}^{Z \to Z}$	generalised collisional-radiative (GCR) excitation coefficient	$m^3 s^{-1}$
$\mathfrak{R}$	Real numbers	
$\mathrm{Var}(f)$	variance of the distribution of f computed by integrating over all variables x_i	
$\mathrm{Var}[Q]$	variance in random variable Q	
m_e	mass of electron	kg

m_i	mass of ion species particle $m_i = Am_u$	kg
m_n	neutral species particle mass	kg
m_p	mass of proton	kg
m_u	atomic mass unit	$1.6605 \times 10^{-27}\,kg$
M_s	Mach number, allowed to take either sign	
M_S	number of energy states of an atom	
μ, ν	(K+S) Dynamic, kinematic viscosities	
$\mu_{cx} = \omega_c/\nu_{cx}$	measures strength of magnetization with respect to charge exchange reaction	
μ_m	reduced mass of two particles	kg
M_Z	number of metastable states for species α (which includes the ground state)	
n	number density	m^{-3}
n_{ref}	reference number density of the plasma ions	m^{-3}
N_{ref}	normalising or reference number density	10^{18}
N	number density, may be scaled by $N_{ref} = 10^{18}$	m^{-3}
n_0	initial number density	m^{-3}
$\nabla\cdot$	(K+S) Divergence	
$\nabla\times$	(K+S) Curl	
∇^2	(K+S) Laplacian	
N_b	(K+S) Number of global boundary degrees of freedom	
$n_B = N/B$	number density divided by field strength	$m^{-3}T^{-1}$
N_D	Number of degrees of freedom per dimension, $D = 1, 2, \ldots 6$	
N_{dof}	(K+S) Number of global degrees of freedom	
n_e	number density of the electrons	m^{-3}
N_{el}	(K+S) Number of finite elements	
N_{eof}	(K+S) Total number of elemental degrees of freedom $N_{eof} \simeq N_{el}N_m$	
n_i	number density of the plasma ions	m^{-3}
$n_j(\mathbf{x}, t)$	member of the set of deterministic coefficients of the "random trial basis"	
N_m	(K+S) Number of elemental degrees of freedom	
n_n	neutral density	m^{-3}
$\notin$	(Sets) Is not a member of; does not belong to	
$\not\subset$	(Sets) Is not a subset of	
n_p	number density of the plasma ions	m^{-3}
N_Q	(K+S) Total number of quadrature points $N_Q = Q_1Q_2Q_3$	
n_s	number density of isotope s	m^{-3}
N_s	number density of isotope s	m^{-3}
N_T	number of samples in temperature used to define typically a crossection in the ADAS database [25, 35]	
ν	plasma kinematic viscosity	m^2s^{-1}
ν_α	kinematic viscosity of species α	m^2s^{-1}
$\nu_{cx} = K_{cx}n_n$	charge exchange 'frequency'	s^{-1}
ν_{e0}	electron kinematic viscosity caused by neutrals	m^2s^{-1}

$\nu_{e\parallel}$		parallel kinematic viscosity of electrons	$m^2 s^{-1}$
$\nu_{e\perp}$		perpendicular kinematic viscosity of electrons	$m^2 s^{-1}$
$\nu_{i\parallel}$		parallel kinematic viscosity of ions	$m^2 s^{-1}$
ν_i		ion kinematic viscosity	$m^2 s^{-1}$
ν_{i0}		ion kinematic viscosity caused by neutrals	$m^2 s^{-1}$
$\nu_{i\perp}$		perpendicular kinematic viscosity of ions	$m^2 s^{-1}$
ν_α^*		(Glossary) Normalised collision frequency for species α	
ν_c^* $\frac{q_e^4}{3m_p^2\epsilon_0^2}L_0 n_0/C_0^4$	=	Collisionality parameter	
ν_α		(Glossary) Collision frequency for species α	s^{-1}
$\nu_{\alpha n}$		Collision frequency for species α with neutrals	s^{-1}
n^Z		number density for charge state Z	m^{-3}
N_Z		number of charge states for an ion species	
n_i^Z		number density for charge state Z, excited state i	m^{-3}
n_σ^Z		number density for charge state Z, metastable state σ	m^{-3}
$\omega_{ce} = |e|B/m_e$		electron cyclotron angular frequency	$radians\,s^{-1}$
$\omega_{ci} = Z_i eB/m_i$		ion cyclotron angular frequency	$radians\,s^{-1}$
$\omega_{pe} = \sqrt{\frac{nq_e^2}{\epsilon_0 m_e}}$		plasma angular frequency for electrons	$radians\,s^{-1}$
$\omega_{pi} = Z_i\sqrt{\frac{nq_e^2}{\epsilon_0 m_i}}$		plasma angular frequency for ions	$radians\,s^{-1}$
Ω		(K+S) Solution domain	
Ω^e		(K+S) Elemental region	
$p(A|B)$		conditional probability of event A given event B is known or assumed to have occurred	
p_α		pressure of species α	Nm^{-2}
$\parallel Q \parallel_E$		the 'energy' norm	
$(\partial f/\partial t)_C$		source in Boltzmann due to inter-particle interactions	$m^{-6}s^2$
$\partial\Omega_e$		(K+S) Boundary of Ω^e	
$\partial\Omega$		(K+S) Boundary of Ω	
$\partial\Omega_{\mathcal{D}}$		(K+S) Domain boundary with Dirichlet conditions	
$\partial\Omega_{\mathcal{N}}$		(K+S) Domain boundary with Neumann conditions	
P_C		number of modes in basis for polynomial chaos	
p_e		pressure of the electrons	Nm^{-2}
ϕ		angle in toroidal direction	radians [c]
Φ		electr(ostat)ic potential	V
ϕ_{pq}, ϕ_{pqr}		(FE Basis) Expansion basis	
$\phi_{e,\xi}$ (FE Basis) expansion basis as a function of global position $\mathbf{x}$			
p		(K+S) pressure	Nm^{-2}
$p = \sum_\alpha n_\alpha k T_\alpha$		plasma pressure	Nm^{-2}
p		as suffix labels (super-)particles	
p_i		pressure of the ion species	Nm^{-2}
P_i		(FE Basis) Polynomial order in the ith direction	

$p(\psi)$	function giving the pressure as a function of ψ of the magnetic flux	Nm^{-2}
p, q, r	(K+S) General summation indices	
Pr	Prandtl number	
Pr_M	magnetic Prandtl number	
ψ	poloidal magnetic flux	Tm^2
$\psi_p^a, \psi_{pq}^b, \psi_{pqr}^c$	(FE Basis) Modified principal functions	
Ψ_i	i^{th} member of a set of basis functions, typically multi-dimensional Hermite polynomials	
$P(T)$	emitted power integrated over all wavelengths	Wm^3
$\mathrm{p}(x)$	probability distributions	
$P(x)$	Cumulant probability distribution	
P^Z	radiated power per atom of n^Z	W
$Q_\parallel$	combined energy flux at a boundary	$Jm^{-2}s^{-1}$
q_α	charge on a particle of species α	C
q_e	charge on an electron	C
$Q(f_\alpha, f_\beta)$	Boltzmann collision operator	$m^{-6}s^2$
Q_H	cooling rate due to excitation as defined in ref [13]	$Km^{-3}s^{-1}$
q_i	charge on an ion	C
$\mathbf{q}_e$	electron energy flux	$Jm^{-2}s^{-1}$
$\mathbf{q}_i$	ion energy flux	$Jm^{-2}s^{-1}$
Q_i	(FE Basis) Quadrature order in the ith direction	
Q_{ie}	collisional energy equipartition term	$kgm^{-1}s^{-3}$
r	order of higher order term	
R	cylindrical coordinate	m
R_0	major radius of torus	m
R_p	recycling coefficient for particles	
R_E	recycling coefficient for particle energy	
ρ	as suffix is label of metastable state	
ρ	(K+S) Density	
$\rho_c = \sum_\alpha Z_\alpha|e|n_\alpha$	charge density of the medium	Cm^{-3}
$\rho_m = \sum_\alpha A_\alpha m_u n_\alpha$	mass density of the medium	kgm^{-3}
$\rho_{t\alpha}$	(Glossary) Gyroradius or Larmor radius of orbit of charged particle of species α about magnetic field direction	m
${}^R\mathcal{F}_{i\sigma}$	coefficient of recombination for the transition from metastable state σ to regular excited state i	
$s_\parallel$	arclength along fieldline	m
s	as suffix, isotope label (α preferred for species)	
s	parameterises distance along the fieldline $0 \le s \le 1$	
S_α	source term in Boltzmann equation for species α	$m^{-6}s^2$
S_C	total source term in Boltzmann equation	$m^{-6}s^2$
$S_{\mathrm{ana}}(\mathbf{x}, t)$	explicit/analytic source term in fluid equation(s)	$m^{-3}s^{-1}$?
$S_{\mathrm{ana}}^n(\mathbf{x}, t)$	numerically convenient source term in fluid equation(s)	$m^{-3}s^{-1}$?
$S_{exp}(\mathbf{x}, \mathbf{v}, t)$	explicit source term in Boltzmann equation	$m^{-6}s^2$
n	neutral density	

T	neutral temperature	
u	neutral velocity	
s_i	arclength parameter for boundary ($i=1$ inner, $i=2$ outer)	
$s^{\mathcal{E}}$	source term in plasma energy equation	
$s_e^{\mathcal{E}}$	energy density source term for electrons	
$s_i^{\mathcal{E}}$	energy density source term for ions	
$s_n^{\mathcal{E}}$	source term in neutral energy equation	
$s_{\perp e}^{\mathcal{E}}$	energy cross-field source term for electrons	
$s_{\perp i}^{\mathcal{E}}$	energy cross-field source term for ions	
$s_{\perp n}^{\mathcal{E}}$	energy cross-field source term for neutrals	
s^{n}	source term in plasma density equation	
s_n^{n}	source term in neutral density equation	
s_e^{n}	number density source term for electrons	
s_i^{n}	number density source term for ions	
s^{u}	source term in plasma momentum equation	
s_n^{u}	source term in neutral momentum equation	
$s_{\perp n}^{u}$	momentum cross-field source term for neutrals	
S_i	Sobol sensitivity index, gives a normalised measure of the sensitivity of the distribution of f to the parameter x_i	
σ	as suffix labels metastable state	
σ	reaction cross-section	m^2
σ_C	reaction rate for charge exchange	
σ_E	cooling rate due to excitation	
σ_E	electrical conductivity	$\Omega^{-1}m^{-1}$
σ_I	reaction rate for ionisation	
$\sigma_s^{i|0}$	collision cross-section for ions with neutrals	m^2
$\sigma_s^{e|0}$	collision cross-section for electrons with neutrals	m^2
S_{ij}	Sobol sensitivity index, gives a normalised measure of the sensitivity of the distribution of f to the parameters x_i and x_j	
$S^{\mathcal{E}}$	source term in plasma energy equation	$kgm^{-1}s^{-3}$
$S_e^{\mathcal{E}}$	energy density source term for electrons	$kgm^{-1}s^{-3}$
$S_i^{\mathcal{E}}$	energy density source term for ions	$kgm^{-1}s^{-3}$
$S_n^{\mathcal{E}}$	source term in neutral energy equation	$kgm^{-1}s^{-3}$
$S_{\perp e}^{\mathcal{E}}$	energy cross-field source term for electrons	$kgm^{-1}s^{-3}$
$S_{\perp i}^{\mathcal{E}}$	energy cross-field source term for ions	$kgm^{-1}s^{-3}$
$S_{\perp n}^{\mathcal{E}}$	energy cross-field source term for neutrals	$kgm^{-1}s^{-3}$
S^{n}	source term in plasma density equation	$m^{-3}s^{-1}$
S_e^{n}	number density source term for electrons	$m^{-3}s^{-1}$
S_i^{n}	number density source term for ions	$m^{-3}s^{-1}$
S_n^{n}	source term in neutral density equation	$m^{-3}s^{-1}$
$S_{\perp n}^{n}$	number density cross-field source term for neutrals	$m^{-3}s^{-1}$
$S_{\perp}^{n}$	number density cross-field source term for plasma	$m^{-3}s^{-1}$
$S_{\perp n}$	generic cross-field source term for neutrals	$m^{-3}s^{-1}$
S^{u}	source term in plasma momentum equation	$kgm^{-2}s^{-2}$

$\subset$	(Sets) Is a subset of	
S_n^u	source term in neutral momentum equation	$kgm^{-2}s^{-2}$
$S_{\perp n}^u$	momentum cross-field source term for neutrals	$kgm^{-2}s^{-2}$
S_ρ^Z	particle source for ion of metastable state σ (species α) with charge state Z	$m^{-3}s^{-1}$
S_α^Z	particle source for ion of species α with charge state Z	$m^{-3}s^{-1}$
t	time usually in seconds	s
t'	offset time usually in seconds	s
T	plasma temperature	eV
t_0	characteristic evolutionary timescale usually in seconds	s
t_s	characteristic timescale usually in seconds	s
t_H	Numerical hand-off time interval usually in seconds	s
t_R	Numerical ramp-up time interval usually in seconds	s
T_0	initial temperature (prefixed by k implies energy in SI)	eV
T_{Kn}	reference temperature of Knudsen distribution (prefixed by k implies energy in SI)	eV
T_{ref}	reference temperature (prefixed by k implies energy in SI)	eV
T_s	characteristic temperature ($T_s = (L_s/t_s)^2/K_M$)	eV
T_α	temperature of species α	eV
τ	optical depth	m
τ_α	collision or relaxation time of species α	s
τ_e	electron collision or relaxation time	s
τ_i	ion species collision or relaxation time	s
τ_{en}	electron-neutral collision time	s
τ_{in}	ion species-neutral collision time	s
$\tau_{ce} = 1/f_{ce}$	electron cyclotron timescale	s
$\tau_{ci} = 1/f_{ci}$	ion cyclotron timescale	s
$\tau_{pe} = 1/f_{pe}$	plasma timescale for electrons	s
$\tau_{pi} = 1/f_{pi}$	plasma timescale for ions	s
$\tau_{\mathcal{E}_e}$	loss time of energy density for electrons	s
$\tau_{\mathcal{E}_i}$	loss time of energy density for ions	s
τ_{n_e}	loss time of number density for electrons	s
τ_{n_i}	loss time of number density for ions	s
$T_d = T_i + T_e$	combined temperature of the electrons and ions	eV
T_e	electron temperature (prefixed by k implies energy in SI)	eV
T_H	the Hydrogen reionisation potential	
θ	angular coordinate	radians [c]
θ	random parameter $0 \le \theta \le 1$	
T_i	ion temperature	eV
$\tilde{a}$	scaled matrix coefficient	
$\tilde{b} = B/B_0$	dimensionless magnetic field	
$\tilde{\psi}_p^a, \tilde{\psi}_{pq}^b, \tilde{\psi}_{pqr}^c$	(FE Basis) Orthogonal principal functions	
u	generic first velocity component	ms^{-1}
U	velocity component (flow) along streamline	ms^{-1}
$U_s = L_s/t_s$	characteristic speed	ms^{-1}
$U_d = L_s/t_0$	speed measuring the importance of the transient term	ms^{-1}

U_A	Alfvén speed	ms^{-1}
$\underline{\boldsymbol{f}}^e$	(K+S) Concatenation of elemental vector $\boldsymbol{f}^e$	
$\underline{\boldsymbol{W}}^e$	(K+S) Block-diagonal extension of matrix $\boldsymbol{W}^e$	
$u_R = 1/R$	Radial component of Grad-Shafranov 'flow'	
v	generic second velocity component	ms^{-1}
V^e	spatial volume occupied by finite element e	m^3
V_i	variance of the distribution of f as the parameter x_i varies	
V_{ij}	variance of the distribution of f as the parameters x_i and x_j vary	
w	generic third velocity component	ms^{-1}
w_{jk}	weight in neural network indexed by neuron j and input k	
w_p	weight of particle p	
$w_{\alpha,ref}$	normalising or reference weight of particle of species α	
w_{ref}	normalising or reference number for superparticles	10^{10}
W	weighting function for particle-in-cell	
x	Cartesian coordinate	m
$x_1, x_2, x_3, \mathbf{x}$	(FE Basis) Global Cartesian coordinates	
x_α	collisionality factor of species α	
$x_e = \omega_{ce}\tau_e$	collisionality factor of electrons	
$x_i = \omega_{ci}\tau_i$	collisionality factor of ions	
x_i	generic parameter or variable	
$\xi_1, \xi_2, \xi_3, \boldsymbol{\xi}$	(FE Basis) Local Cartesian coordinates	
ξ_i	random number within the unit interval $[0,1]$	
$^X\mathcal{F}_{i\sigma}$	coefficient of excitation for the transition from metastable state σ to regular excited state i	
y	Cartesian coordinate	m
z	Cartesian coordinate	m
Z	Cartesian coordinate	m
Z	charge state of the ion	
Z	cylindrical coordinate	m
$Z_0(\alpha)$	number of charge states of species α included in the model	
Z_a	Gaussian random process, index a	
ζ	magnetic Prandtl number as defined in Cambridge	
$\zeta = -\phi$	toroidal angle coordinate	radians [c]
Z_i	charge state	
$Z_m = Z - 1$	where Z is ion charge state	
$Z_p = Z + 1$	where Z is ion charge state	
$Z_{sum} = \sum_\alpha Z_0(\alpha)$	where Z_0 is number of charge states of species α	